T.&A.M. Report No. 496

The relation between curvature, rate state-dependence and detonation velocity**

Rupert Klein*and D. Scott Stewart†

November 28, 1990

Abstract

The paper considers the effect of rate state - dependence and curvature on detonation velocity and detonation structure in the quasi - steady quasi-onedimensional limit. Extensions of prior results of Bdzil and Stewart as well as the correct analysis of the problem for Arrhenius kinetics, originally considered by Wood and Kirkwood, are given. New formulas for large activation energy are obtained. The latter half of the paper provides a derivation of the relevant front evolution equations and of the simplified asymptotic equations using Whitham's shock ray coordinates.

Keywords: Near-CJ detonation, curvature effects, rate state dependence

AMS (MOS) subject classification: 76L05, 76H05

1 Introduction

The history of the relation between detonation velocity and the radius of curvature of the detonation shock has its origins in the work of Wood and Kirkwood, [1]. In their classic paper they considered the central streamtube for a steady, curved detonation with a locally symmetric detonation shock. The analysis is a structure analysis of a quasi-one-dimensional ZND detonation and assumes that the shock has weak curvature and is traveling close to the Chapman Jouguet (CJ) velocity. In particular, they showed that the wave had to obey a "generalized Chapman-Jouguet condition" at a point

*Institut für technische Mechanik, RWTH Aachen, Templergraben 64, 5100 Aachen, Germany

†Theoretical and Applied Mechanics, University of Illinois, Urbana, Illinois, 61801

**Submitted to SIAM Journal of Applied Mathematics

imbedded in the reaction zone behind the detonation shock. In the language used here this condition is derived by finding the common zeroes of the *thermicity* and *sonic* functions. For simple exothermic reactions, the generalized CJ - condition is satisfied only for diverging waves.

Having reduced the problem to solving the ODE's through the reaction zone, which must satisfy the shock boundary conditions and the generalized CJ condition, Wood and Kirkwood attempted to illustrate a specific example of the detonation velocity - curvature relation by choosing a depletion rate law with Arrhenius kinetics, namely

$$R \sim (1-\lambda)^{\nu} e^{-E^*/RT}, \tag{1}$$

where λ measures the extent of reaction, ($\lambda = 1$ at completion). An ad hoc analysis followed where a discontinuous, square wave structure was assumed with the conclusion that the relation between the normal detonation shock velocity, D_n, and the curvature, κ was linear. (However, their result for the difference $D_n - D_{CJ}$ is multiplied by an undetermined 'constant', which can be inferred to be a function of the curvature, but it is not explicitly given, nor is it clear how to identify it from their analysis.) An exact analysis of their equations was not given.

Nevertheless, their work represents a fundamental contribution to detonation theory because it demonstrated that a relation between the detonation velocity and the curvature might exist and showed a theoretical pathway which has finally led to a rigorous derivation of the result.

In 1981, Bdzil, [2], considered the problem of a steady-state detonation propagating down the axis of a cylindrical stick of finite radius. His perturbation analysis was based on the assumption that the length scales of the detonation geometry are much larger than a typical reaction zone thickness. The result was a second order differential equation for the shock locus which, when solved subject to a confinement boundary condition, provided a relation between the axial, steady detonation velocity and the charge diameter. This was the first systematic derivation of the *diameter effect* observed in condensed phase explosives. His calculations in [2] used a special rate law, chosen somewhat for analytical convenience. Although it was not explicitly stated in this paper, the equation for the shock locus is equivalent to a linear relation between the normal shock velocity and the local shock curvature.

Stewart and Bdzil published a paper in 1988, [3], where they demonstrated that a quasi-steady relation between D_n and κ exists and that the functional form of the relation depends in detail on the equation of state and the rate law. In some cases the $D_n - \kappa$ relation is linear, but for $\nu = 1$ and $E^* = 0$, (say), the leading order correction to the detonation shock velocity is logarithmic. This result has led to evolution equations that predict the dynamics of motion of the detonation shock for a class of important detonation flows.

This paper extends some of these results obtained previously by Stewart and Bdzil and considers the case of Arrhenius kinetics in detail. We also extend the accuracy of the results, providing new formulas for $1/2 < \nu \leq 1$. In the second half of the paper we give a careful derivation of the equations of motion in terms of front attached coordinates. The equations are analyzed to justify the quasi-onedimensional quasisteady approach for diverging waves. They also provide the basis for further theoretical developments.

Motivation for this work comes from several sources. First, the $D_n - \kappa$ *relation* has been recognized as the basis for a new principle of explosive design called *Detonation Shock Dynamics* by Bdzil and Stewart after Whitham's Geometrical Shock Dynamics, [4],[5],[6],[7]. This is very much a practical concern as the *method* of Detonation Shock Dynamics may reduce the time and effort required to design explosive components. It is asserted that the $D_n - \kappa$ relation is an intrinsic property of the explosive and hence directly measurable by experiment. Thus our present calculations are important for the purpose of cataloging how different assumed forms of the rate law generate different $D_n - \kappa$ curves.

A second motivation for this work is for enhanced theoretical understanding of multidimensional detonation within the context of a standard model problem of gas-phase detonation, the Euler equations with an ideal equation of state and a single exothermic reaction with Arrhenius kinetics. The solutions given here represent steady and a certain class of unsteady, multidimensional solutions. Also, the steady solutions are the basis for further systematic linear stability studies, following Lee and Stewart [8].

In Section 2., using the end results of Sections 5.-7., we give the relevant formulation of the divergent detonation problem which is essentially equivalent to that posed originally by Wood and Kirkwood. Section 3. derives the asymptotic results based on the formulation in Section 2. for a rate

law with a general and unspecified state-dependent rate constant. Section 4. considers the particular form of the formulas for an Arrhenius rate constant and examines the relative effects of the increased depletion dependence, ν, and rate state-dependence. Explicit formulas are given in the limit of large activation energy. Sections 5.-7., in detail, illustrate all the assumptions used to derive the equation set of Section 2. Starting from Whitham's shock ray coordinates, [9], in Section 5., we provide special results for two dimensions in Sections 6,7. We explain the front evolution equations under a D_n-κ law in the shock ray coordinates in Section 6. and give a justification of the quasisteady quasi-onedimensional equations of Sections 2.-4. in Section 7.

2 The reduced problem

The governing equations are the Euler equations with reaction, written in a shock-attached intrinsic coordinate frame. Section 5. uses Whitham's shock ray coordinates. The approximations used in our analysis assume that the detonation shock travels along its normal at a velocity close to the CJ value and that its radii of curvature are very large compared to a typical reaction zone thickness. It is assumed that the flow is nearly 1-D and quasi-steady. Restrictions are placed on this theory in the sense that the terms neglected must be uniformly small. Estimates for the various terms in the full governing equations are given in Section 7.

To the order needed for our analysis, the (dimensional) equations are consistently written as,

$$\frac{\partial \rho u}{\partial n} + \kappa \rho (u + D_n) = 0, \tag{2}$$

$$u\frac{\partial u}{\partial n} + \frac{1}{\rho}\frac{\partial P}{\partial n} = 0, \tag{3}$$

$$\frac{\partial E}{\partial n} - \frac{P}{\rho^2}\frac{\partial \rho}{\partial n} = 0, \tag{4}$$

$$u\frac{\partial \lambda}{\partial n} = r. \tag{5}$$

In the above, ρ ,u, D_n, P, E, λ and r represent the density, normal particle velocity relative to the shock, the normal detonation velocity, pressure, specific internal energy, reaction progress variable and the reaction rate. The variable κ, is the sum of the principal curvatures of the detonation shock surface. The variable n is essentially the distance normal to the detonation shock.

The governing equations required for this section are completed by specifying the equation of state $E(P, \rho, \lambda)$ and the rate law, $r(P, \rho, \lambda)$. Here we take E to correspond to a polytropic fluid, or an ideal gas, thus

$$E = \frac{1}{\gamma - 1}\frac{P}{\rho} - Q\lambda \qquad \text{and} \qquad r = K(P, \rho)(1 - \lambda)^{\nu}, \tag{6}$$

and later we take $K = ke^{-E^*/RT}$ for Arrhenius kinetics. In equation (6), Q is the specific heat of reaction, γ is the polytropic exponent, K and k are rate constants, ν is a depletion exponent and E^* is an activation energy. The temperature T is identified by an ideal thermal equation of state, so that $T = P/\rho R$. The sound speed is $c^2 = \gamma P/\rho$.

To these equation we add the strong shock relations

$$\begin{aligned} -\rho_- D_n &= \rho_+ u_+, \qquad P_+ = \rho_- D_n(u_+ + D_n), \\ \frac{D_n^2}{2} &= E_+ + \frac{P_+}{\rho_+} + \frac{u_+^2}{2}, \qquad \lambda_+ = 0. \end{aligned} \tag{7}$$

The " $-$ " subscript refers to the state ahead of the shock, the " $+$ " subscript to the state behind the shock. We have used the strong shock approximation, which simplifies the shock relations, and neglects the terms proportional to P_-, relative to the shock pressure. One can show that the total enthalpy is conserved throughout the structure,

$$H = \frac{c^2}{(\gamma - 1)} + Q(1 - \lambda) + \frac{u^2}{2} = \frac{D_n^2}{2} + Q. \tag{8}$$

In the strong shock approximation, [3], the following formula for D_{CJ} holds,

$$D_{CJ}^2 = 2Q(\gamma^2 - 1). \tag{9}$$

In order to simplify the subsequent discussion we scale the density, with ρ_-, the pressure with $\rho_- D_{CJ}^2$ and the velocity with D_{CJ}. A natural length scale for plane detonation is the 1-D reaction zone thickness which can be represented as a characteristic reaction time, t_c, times D_{CJ}. Thus the characteristic length is $D_{CJ}t_c$. It will turn out that the natural choice for t_c is proportional to the inverse of the reaction rate constant evaluated at the end of the reaction zone near the sonic point. This characteristic time arises naturally when the *generalized CJ condition* is imposed. An explicit representation for t_c is given in section 2.1, (22).

Another characteristic length is related to the (reference) curvature κ_0. The inverse of the reference curvature is typically the width of a confining tube or is of the dimension of the combustion device. The ratio of these disparate lengths defines a natural perturbation parameter

$$\delta = (D_{CJ}t_c)\kappa_0 << 1, \tag{10}$$

and the assumption of small curvature is then explicitly written as

$$D_{CJ}t_c\kappa < \delta << 1. \tag{11}$$

Thus, the dimensionless curvature, κ, that appears in the following equations can be used as an expansion parameter and its size is directly controlled by δ. Note that the reaction zone length is usually quite small on a laboratory measurement scale, so that considerable or even strong curvature on the scale of the combustion device is not necessarily excluded by our discussions.

The governing equations, are unchanged under this scaling and from now on quantities are considered to be dimensionless: dimensional quantities will be referenced with a tilde superscript. The reaction rate that appears is $r = \tilde{r}\tilde{t_c}$. Equation (4) can be replaced by equation (8) which is rewritten as

$$\frac{\gamma}{(\gamma-1)}\frac{P}{\rho} + \frac{u^2}{2} - q\lambda = \frac{D_n^2}{2}, \tag{12}$$

where

$$q \equiv \frac{\tilde{Q}}{\tilde{D_{CJ}^2}} = \frac{1}{2(\gamma^2-1)}. \tag{13}$$

The shock conditions, solved explicitly in terms of D_n, are

$$
\begin{aligned}
u &= -\frac{(\gamma-1)}{(\gamma+1)} D_n \,, \qquad \rho = \frac{\gamma+1}{\gamma-1} \,, \\
P &= \frac{2}{\gamma+1} D_n^2 \,, \qquad \lambda = 0 \qquad \text{at } n = 0.
\end{aligned} \tag{14}
$$

The problem posed by (2), (3), (12), (5) and (14) is essentially in the same form as that posed by Wood and Kirkwood.

Instead of solving the problem in the wave coordinate, the problem is conveniently reduced to the analysis of a single equation in the $u - \lambda$ phase-plane. (This form of the presentation can first be found in Fickett and Davis [10].) In Section 5. a more general version of this *master equation* is derived which includes all terms due to unsteadiness and multidimensionality. One can simply derive this equation by differentiating (12) and eliminating P and ρ explicitly in terms of u and λ, thus obtaining

$$
\frac{du}{d\lambda} = \frac{u[q(\gamma-1)r - c^2\kappa(u+D_n)]}{r(c^2-u^2)} \equiv \frac{u}{r}\frac{\phi}{\eta}, \tag{15}
$$

where

$$
c^2 = \frac{(\gamma-1)}{2}\left[D_n^2 - u^2 + 2q\lambda\right], \tag{16}
$$

with the shock boundary condition given by (14a).

In what follows, we define the thermicity locus by

$$
\phi \equiv q(\gamma-1)r - c^2\kappa(u+D_n) = 0, \tag{17}
$$

and the sonic locus will be defined by

$$
\eta \equiv c^2 - u^2 = 0. \tag{18}
$$

(The definitions of thermicity and the sonic loci differ slightly from those found in Fickett and Davis, but share the same zeroes.)

In general, solutions to the above problem become singular near a sonic point, $\eta = 0$. For solutions to be admissible, ϕ and η have to pass through a common zero which exists only if there is a particular relation between D_n and κ. We derive this relation explicitly by asymptotics in κ. Anticipating

that $u + D_n$ is positive throughout the reaction zone, we observe that a zero of ϕ can only appear if κ is positive, i.e., in a diverging wave. For converging waves, the present approach is not directly applicable. For a discussion of the converging wave problem, the reader is referred to Klein, [11].

2.1 The location of the critical points in the u-λ plane (the generalized CJ condition)

An admissible solution of (15) must satisfy both the shock boundary condition and the critical point criterion, that η and ϕ vanish simultaneously. For arbitrary pairs of D_n and κ the differential problem is overdetermined. Both conditions are satisfied only if a relation, $D_n = D_n(\kappa)$, between the curvature and detonation speed exists. That such a relation always exists is not proven. When it does exist, the relation depends on the particular form of the energy function, $E(P, \rho, \lambda)$, and of the reaction rate function, $r(P, \rho, \lambda)$.

The critical points of (15), in the u-λ plane, define the generalized CJ-condition described by Wood and Kirkwood [1], although equation (15) does not appear there. In the u-λ plane, the task is to integrate from the shock, through the critical point that is imbedded in the reaction zone. If we think of D_n as being fixed (say), then the starting point of an integration and the trajectory of the solution will be determined, but unless κ has a specific value, the trajectory will not pass through the critical point. Ensuring that it does so, determines the $D_n - \kappa$ relation (also see Fickett and Davis' discussion of slightly divergent detonation in the $u^2 - \lambda$ plane, [10]).

Recall that the critical points are defined by the roots of the thermicity and sonic parameters, ϕ and η, respectively. Consequently, if $\kappa << 1$ then $r << 1$ and hence $(1 - \lambda) << 1$ and the critical points must be near the line of complete reaction, $\lambda = 1$, and hence near the plane CJ state. Given κ and $D_n' \equiv D_n - 1$, one can determine the location of the critical point in the $u - \lambda$ plane to leading order from (17) and (18). First the thermicity condition, $\phi = 0$, yields

$$\lambda_{cr}' = (1 - \lambda)_{cr} = \left[\frac{c^2(u + D_n)}{q(\gamma - 1)K}\right]_{CJ}^{1/\nu} \kappa^{1/\nu} + \ldots \equiv s_* \kappa^{1/\nu} + \ldots . \qquad (19)$$

The value of u^2 at the critical point is then obtained from the sonic

condition $(c^2 - u^2)_{cr} = 0$ and from the expression, (16), for the speed of sound. We find

$$c_{cr}^2 = u_{cr}^2 = \frac{\gamma^2}{(\gamma+1)^2} + 2\frac{\gamma-1}{\gamma+1}D_n' - \frac{1}{(\gamma+1)^2}\lambda' + O(\lambda'^2, D_n'^2). \tag{20}$$

Using the leading order values of the solution to evaluate s_* shows

$$s_* = \left[\frac{2\gamma^2}{(\gamma+1)^2 K_{CJ}}\right]^{1/\nu}. \tag{21}$$

So far, the parameter K_{CJ} appears and is the value of the dimensionless rate constant, $K \equiv \tilde{K}\tilde{t}_c$, evaluated at the CJ end state. For convenience, we choose the time scale so that $s_* \equiv 1$, i.e., we let

$$K_{CJ} = \frac{2\gamma^2}{(\gamma+1)^2} \qquad \text{or} \qquad \tilde{t}_c = \frac{2\gamma^2}{(\gamma+1)^2}\tilde{K}_{CJ}^{-1}. \tag{22}$$

In this way, the inverse of the reaction rate constant evaluated at the CJ end state is the *natural* time scale, $\tilde{t}_c$, mentioned below (9).

Notice that the order of λ_{cr}' is a noninteger power of κ unless $1/\nu$ is integer. Also, the order of λ_{cr}' satisfies the estimates

$$\begin{aligned} &\kappa >> \kappa^2 >> \kappa^{1/\nu}, \quad \text{for} \quad 0 < \nu < 1/2 \\ &\kappa >> \kappa^{1/\nu} >> \kappa^2, \quad \text{for} \quad 1/2 < \nu < 1, \end{aligned} \tag{23}$$

suggesting that a straight-forward expansion in terms of integer powers of κ might not be second order accurate in the latter regime for ν. In fact, we will show that it is necessary to perform a multiple power expansion in order to follow the solutions through the critical point.

3 Asymptotic analysis

3.1 The Main Reaction Layer

The flow behind the detonation shock breaks into two layers, a main reaction layer (MRL) in which most of the combustion occurs and a region very near

the sonic point and near reaction completion which we call the transonic layer (TSL), (See [3] for $\nu = 1$ and [11]). In the following, we adopt the convention that a capital U will be used to represent the velocity in the MRL while a lower case u will be used in the TSL. When no distinction is necessary, u will be used.

In the regions of the $u - \lambda$ plane, where the curvature term in (15) is small compared to the chemical source term, the leading order structure is that of a plane CJ - ZND wave. The plane CJ solution is conveniently expressed in terms of the variable

$$\ell = \sqrt{1 - \lambda} \tag{24}$$

and is given by

$$u(\ell) = -\frac{\gamma - \ell}{\gamma + 1}, \qquad P(\ell) = \frac{1 + \ell}{\gamma + 1}, \qquad \rho(\ell) = \frac{\gamma + 1}{\gamma - \ell}, \tag{25}$$

where the distribution of the reactant is found from the integral of the rate equation,

$$n = \int_{\ell}^{1} \frac{u(\hat{\ell})}{r(P, \rho, 1 - \hat{\ell}^2)} 2\hat{\ell}\, d\hat{\ell}. \tag{26}$$

In the MRL, the leading order approximation of the velocity, $u \equiv U$, follows from an integration of (15) neglecting the curvature and using the shock condition. Notice that the rate function drops out of this calculation.

Next we construct the first order correction to this solution in the MRL. The shock boundary conditions require that the largest perturbations of $u \equiv U$ and D_n be comparable. Thus the MRL expansions must take the form

$$u = U^{(0)}(\ell) + U' + \ldots, \qquad D_n = 1 + D_n' + \ldots, \tag{27}$$

where $U^{(0)}$ is given by (25a). The asymptotic orders of U', D_n' as $\kappa \to 0$ are not yet specified. As we will see, they will ultimately be determined by matching the solutions in the MRL and TSL.

We insert these expansion into equation (15) and the shock condition (14a) to obtain a differential equation for U'. The effects of small curvature, relative to the leading perturbations in the MRL are uniformly accounted for,

so long as $\kappa/U' \sim O(1)$ or smaller, as $\kappa \to 0$. Thus we obtain the following problem,

$$\begin{aligned} \frac{dU'}{d\ell} + \frac{\gamma}{\ell(\gamma-\ell)} U' &= -\frac{\gamma-1}{\ell(\gamma-\ell)} D_n' - \frac{\kappa}{\gamma(\gamma+1)} \frac{(\gamma-\ell)(1+\ell^2)}{\ell^{2\nu}} \frac{K^{(0)}(0)}{K^{(0)}(\ell)}, \\ U' &= -\frac{\gamma-1}{\gamma+1} D_n' \text{ at } \ell = 1, \end{aligned} \tag{28}$$

with the solution given by

$$U' = -\frac{D_n'}{\gamma+1}\left(\gamma - \frac{1}{\ell}\right) - \kappa \frac{1}{(\gamma+1)}\left(\frac{1}{\gamma} - \frac{1}{\ell}\right) \int_\ell^1 F(\ell)\, d\hat{\ell}\,. \tag{29}$$

where

$$F(\ell) \equiv \frac{(1+\ell)^2\, \ell^{1-2\nu}}{K^{(0)}(\ell)/K^{(0)}(0)}. \tag{30}$$

In general, the approximation $u = U^{(0)} + U' + O(U'^2)$ is not uniformly valid as $(\ell \to 0)$. The first obvious improvement is to eliminate the strongest singularity proportional to $1/\ell$ by choosing $D_n' = -\kappa \int_0^1 F(\ell)\, d\ell$. The behavior of U' then depends on the limit

$$\frac{1}{\ell}\left[\int_\ell^1 F(\hat{\ell})\, d\hat{\ell} - \int_0^1 F(\ell)\, d\ell\right] = O(\ell^{1-2\nu}) \qquad \text{as} \qquad (\ell \to 0). \tag{31}$$

For $0 \le \nu \le 1/2$, U' is bounded, but for $1/2 < \nu < 1$ the solution diverges as $\ell \to 0$. This divergence can only be resolved by matching with the boundary layer solution of the TSL near $\ell = 0$. In this layer, the order of the perturbation changes.

For the case of simple depletion, $\nu = 1$, the integral that would normally, define the leading term in D_n, i.e., $\int_\ell^1 F(\hat{\ell}) d\hat{\ell}$, diverges logarithimically as $\ell \to 0$. Even in the MRL, the leading order correction is no longer $O(\kappa)$. The case of $\nu = 1$, for a constant rate coefficient was analyzed in [3] and the generalization is given in Section 3.4 below.

3.2 The transonic layer expansion scheme

Since we assume the detonation to travel at nearly the Chapman-Jouguet velocity, the state at the end of the reaction zone is close to CJ conditions. From considerations of the leading order matching of solutions in the MRL and the TSL, we can motivate the following structure argument for the solution in the TSL of the form,

$$u = -\frac{\gamma}{\gamma+1} + g(\kappa)u^{(g)}(s) + \ldots, \qquad D_n = 1 + o(g), \tag{32}$$

where

$$\lambda = 1 - h(\kappa)s, \tag{33}$$

and $g(\kappa)$ and $h(\kappa)$ are as yet undetermined gauge functions. By comparison with (19) the location of the critical point is at $s = s^* = 1$, if $h = \kappa^{1/\nu}$.

By inserting the above expansions in (15), one obtains the following equation for $u^{(g)}$

$$u^{(g)}\frac{du^{(g)}}{ds} = \left(\frac{h}{g^2}\right)\frac{1}{2(\gamma+1)^2}\left[1 - \frac{2\gamma^2}{(\gamma+1)^2}\frac{\kappa}{r}\right]. \tag{34}$$

Unless $h/g^2 = O(1)$, (the constant of proportionality we can choose to be one) and κ/r is at most O(1) in the TSL, it is not possible to match the corresponding TSL expansion (32) with the limiting form of the MRL expansion. This argument suggests a relation between the thickness of the TSL and the size of the perturbation. Also the order of the perturbation of detonation velocity, is smaller than the u - perturbation, i.e., as long as D_n' is $o(g)$, it does not enter the TSL structure through $O(g)$. In contrast, the perturbations of D_n and U are comparable in the MRL layer, since the MRL solution must satisfy the shock relations at $l = 1$. Note that the outer limits of the inner TSL solution will induce higher order terms that must be in the MRL expansion, thus dictating the form of the MRL expansions.

Thus the natural choice for the scaling function for the TSL is $(h/g^2) = 1$. The size of h and g in terms of κ is then obtained by requiring that the curvature and chemical source terms in the Master equation directly compete in the TSL, which is guaranteed if $h = \kappa^{1/\nu}$, and $\kappa/r = O(1)$. Then the outer

limit of the TSL expansion generates a term that matches with the $1/\ell^{2\nu-1}$ of the inner limit of the MRL expansion. Thus, the appropriate scalings are

$$h(\kappa) = \kappa^{1/\nu} \qquad \text{and} \qquad g(\kappa) = \kappa^{1/2\nu}. \tag{35}$$

3.3 The regime $0 \leq \nu < 1$

According to the discussion in section 3.2, if we seek a solution in the transonic layer of the form

$$u = -\frac{\gamma}{\gamma+1} + \kappa^{1/2\nu} u^{(1/2\nu)}(s) + o(\kappa^{1/2\nu}), \tag{36}$$

where

$$s = \kappa^{-1/\nu}(1-\lambda), \tag{37}$$

then (34) becomes

$$\frac{\partial u^{(1/2\nu)^2}}{\partial s} = \frac{1}{(\gamma+1)^2}\left(1 - \frac{1}{s^\nu}\right). \tag{38}$$

Since $(c^2 - u^2)^{(1/2\nu)} \sim u^{(1/2\nu)}$, the critical point is defined by

$$u^{(1/2\nu)} = 0 \qquad \text{at} \qquad s = 1. \tag{39}$$

The solution for $u^{(1/2\nu)}$ is

$$u^{(1/2\nu)}(s) = \frac{1}{\gamma+1}\left[s - 1 - \frac{s^{1-\nu}-1}{1-\nu}\right]^{1/2}. \tag{40}$$

To match the TSL and the MRL solutions, we replace s with ℓ, using the definition $s = \kappa^{-1/\nu}\ell^2$, to obtain the large-$s$ limit of the TSL solution, and compare with the small - ℓ limit of the MRL solution. In particular we find, starting with the TSL solution that

$$\begin{aligned} \lim_{s\to\infty} u \;&=\; -\frac{\gamma}{\gamma+1} + \frac{1}{\gamma+1}\left[\ell - \frac{\kappa}{2(1-\nu)}\frac{1}{\ell^{2\nu-1}}\right. \\ &+\; \left.\frac{\kappa^{1/\nu}\nu}{2(1-\nu)}\frac{1}{\ell} + \kappa^{1/2\nu} O(s^{-2\nu}, s^{-2})\right]. \end{aligned} \tag{41}$$

The small-ℓ version of the MRL solution is

$$\lim_{\ell\to 0} U = -\frac{\gamma}{\gamma+1} + \frac{1}{\gamma+1}\left[\ell + \frac{1}{\ell}\left\{D_n' + \kappa\int_0^1 F(\hat{\ell})d\hat{\ell}\right\} - \frac{\kappa}{2(1-\nu)}\frac{1}{\ell^{2\nu-1}} + O(D_n', \kappa, \kappa\ell^{2-2\nu})\right]. \tag{42}$$

We observe that the term proportional to $1/\ell^{2\nu-1}$, which is generated from (31), automatically matches a corresponding term in the TSL expansion. Comparison of all terms proportional to $1/\ell$ reveals that the detonation speed perturbation is given by (writing out $F(\ell)$ from (30))

$$D_n' = -\kappa\int_0^1 \frac{(1+\hat{\ell})^2\,\hat{\ell}^{1-2\nu}}{K^{(0)}(\ell)/K^{(0)}(0)}\,d\hat{\ell} + \kappa^{1/\nu}\,\frac{\nu}{2(1-\nu)}\,, \tag{43}$$

which is valid up to order $O(\kappa^2)$. Notice that the correction to order $O(\kappa^{1/\nu})$ could have been neglected entirely when $\nu \le 1/2$. The leading order correction to the detonation velocity, which is linear in the curvature, is the result originally obtained by Stewart and Bdzil, in [3]. As we let $\nu \to 1$, the first as well as the second term in D_n' diverges and a modification of the solution with the introduction of logarithmic terms is required.

3.4 The regime $\nu = 1$

Here we give the simple depletion result, which extends the results of Stewart and Bdzil when $\nu = 1$. As $\nu \to 1$, the description in the TSL becomes singular as apparent from (43). Equation (38) shows the resolution since when $\nu = 1$, logarithms are produced by the solution. It is easy to argue that if the TSL expansion is given by (36) with $\nu \equiv 1$, then the outer limit of the TSL induces an expansion in the MRL of the form

$$U = \frac{\ell-\gamma}{\gamma+1} + \kappa\ln\kappa U^{(\ln)} + \kappa U^{(1)} + \dots\,,$$
$$D_n = 1 + \kappa\ln\kappa D_n^{(\ln)} + \kappa D_n^{(1)} + \dots\,. \tag{44}$$

The derivation in section 3.1 is general enough that we may simply insert $D_n' = \kappa\ln\kappa D_n^{(\ln)} + \kappa D_n^{(1)} + \ldots$ into (29) to obtain the desired result. For the

purpose of matching to the TSL we need the limit of the MRL solution as $\ell \to 0$, which is

$$\begin{aligned} U &= \frac{\ell-\gamma}{\gamma+1} + \frac{\kappa \ln \kappa}{\ell(\gamma+1)} D_n^{(\ln)} \\ &+ \frac{\kappa}{\ell(\gamma+1)} \left\{ D_n^{(1)} + \left[\frac{5}{2} - \ln \ell + \int_0^1 \frac{(1+\ell)^2}{\ell} \left(\frac{K^{(0)}(0)}{K^{(0)}(l)} - 1 \right) dl \right] \right\} \\ &+ O(\kappa \ln \kappa). \end{aligned} \tag{45}$$

The TSL expansion (using the solution found by setting $\nu = 1$ in (38) for $u^{(1/2)}$) is

$$u = -\frac{\gamma}{\gamma+1} + \kappa^{1/2} \frac{1}{\gamma+1} [s - 1 - \ln(s)]^{1/2} + O(\kappa \ln \kappa), \tag{46}$$

which leads to the large-s representation of the velocity

$$u = -\frac{\gamma}{\gamma+1} + \kappa^{1/2} \frac{s^{1/2}}{\gamma+1} \left(1 - \frac{1}{2} \frac{\ln s}{s} - \frac{1}{2s} + O([\ln s/s]^2) \right). \tag{47}$$

Rewriting this last result, using $s^{1/2} = \kappa^{-1/2} \ell$, we find

$$u = \frac{\ell-\gamma}{\gamma+1} + \frac{1}{2(\gamma+1)} \frac{\kappa \ln(\kappa)}{\ell} - \frac{\kappa}{\ell(\gamma+1)} \left\{ \frac{1}{2} + \ln(\ell) \right\} + O(\kappa^{1/2} \frac{\ln^2(s)}{s^{3/2}}). \tag{48}$$

Comparison of the the MRL and TSL expansions reveal that the logarithmic term $\kappa \ln(\ell)/\ell$ is automatically matched and that the detonation speed perturbation is

$$D_n' = \frac{\kappa \ln \kappa}{2} - \kappa \left[3 + \int_0^1 \frac{(1+\ell)^2}{\ell} \left(\frac{K^{(0)}(0)}{K^{(0)}(\ell)} - 1 \right) d\ell \right]. \tag{49}$$

This extends the result given by Stewart and Bdzil to include additional reaction rate, state-dependence. In their work the rate coefficient, K, was constant, in which case the integral contribution to order κ in (49) does not appear.

A remark on the matching procedures for the regimes $\nu < 1$ and $\nu = 1$ is in order: For $\nu < 1$, we needed only the leading order perturbation $u^{(1/2\nu)}$

in the TSL to match all the diverging terms, as $\ell \to 0$, from the first order MRL solution. Similarly, the first order MRL solution was sufficient to cover all the divergences of $u^{(1/2\nu)}$ as $s \to \infty$. A detailed calculation shows that the situation changes for $\nu = 1$. To match a $\kappa \ln \ell$ - divergence in the MRL solution, one needs perturbations of order $\kappa \ln \kappa$ and $\kappa \ln s$ in the TSL. While the first term is straight forwardly derived form the a linearized version of (38) with $\nu = 1$, the latter requires a second order solution in the TSL. It suffices to say that result of this analysis do not change the leading order results for $D_n(\kappa)$.

3.5 Summary

In this section we summarize the results of section 3. by listing the formulas for D_n and the 2-2 composite expansions, [12], accurate to $O(\kappa)$ for the particle velocity u for the various cases considered. First define the integrals

$$I_1(\ell) \equiv \int_\ell^1 \frac{\ell^{1-2\nu}(1+l)^2}{K^{(0)}(l)/K^{(0)}(0)} dl, \qquad I_2(\ell) \equiv \int_\ell^1 \frac{(1+l)^2}{\ell} \left(\frac{K^{(0)}(0)}{K^{(0)}(l)} - 1 \right) dl, \tag{50}$$

then we have found,

$0 \leq \nu < 1$

$$D_n = 1 - \kappa I_1(0) + \kappa^{1/\nu} \frac{\nu}{2(1-\nu)} + O(\kappa^2), \tag{51}$$

$$\begin{aligned} u^{(c)} &= \frac{\ell - \gamma}{\gamma + 1} + \frac{\kappa^{1/2\nu}}{\gamma + 1} \left\{ \left[s - 1 - \frac{s^{1-\nu} - 1}{1-\nu} \right]^{1/2} - s^{1/2} \right\} \\ &+ \frac{\kappa}{\gamma + 1} \left\{ \frac{1}{\ell} [I_1(\ell) - I_1(0)] + \frac{\ell^{1-2\nu}}{2(1-\nu)} \right\} - \kappa^{1/\nu} \frac{\gamma}{2(\gamma+1)} \frac{\nu}{(1-\nu)} \\ &- \frac{\kappa}{\gamma(\gamma+1)} I_1(\ell). \end{aligned} \tag{52}$$

for $\kappa^{1/2\nu} \leq \ell \leq 1$.

$\nu = 1$

$$D_n = 1 + \frac{\kappa \ln \kappa}{2} - \kappa \left[3 + I_2(0)\right] + \ldots \tag{53}$$

$$\begin{aligned} u^{(c)} &= \frac{\ell - \gamma}{\gamma + 1} + \frac{\kappa^{1/2}}{\gamma + 1}\left\{[s - 1 - \ln s]^{1/2} - s^{1/2}\right\} \\ &+ \frac{\kappa}{(\gamma + 1)}\left[\left(\gamma - \frac{1}{\ell}\right)\left[3 + I_2(0)\right] - \left(\frac{1}{\gamma} - \frac{1}{\ell}\right) I_1(\ell) + \frac{1}{2\ell} + \kappa \frac{\ln \ell}{\ell}\right] \\ &- \kappa \ln \kappa \frac{\gamma}{2(\gamma + 1)}. \end{aligned} \tag{54}$$

for $\kappa^{1/2} \leq \ell \leq 1$.

4 Arrhenius kinetics

A standard model for the state-dependent rate is that of Arrhenius kinetics. A dimensional Arrhenius reaction rate constant is given by

$$\tilde{K} = \tilde{k} e^{-\tilde{E}^*/\tilde{R}\tilde{T}}. \tag{55}$$

The dimensionless activation energy is defined as $\theta = \tilde{E}^*/\tilde{R}\tilde{T}_c$ based on the characteristic temperature, $\tilde{T}_c = \tilde{D}_{CJ}^2/\tilde{R}$, which is on the order of the shock temperature. Thus the rate constant at the end of the reaction zone is $\tilde{K} = \tilde{k} \exp\left(-\theta/T_{CJ}\right)$, where T_{CJ} is the dimensionless temperature at the end of the reaction zone. According to the formulas of Section 3.5, the rate state - dependence of our results appears through the integrals $I_1(l)$ and $I_2(l)$. In these expressinos, K must be evaluated with the leading order temperature $T^{(0)}$, which is given by (now dropping the scripts)

$$\frac{1}{T(\ell)} = \frac{(\gamma + 1)^2}{(\gamma - \ell)(1 + \ell)}. \tag{56}$$

Thus the formula for the scaled rate constant, K, is

$$K = \frac{2\gamma^2}{(\gamma + 1)^2} e^{\theta[1/T(0) - 1/T(\ell)]} \tag{57}$$

and the integrals $I_1(\ell)$ and $I_2(\ell)$ become

$$I_1(\ell) = \int_\ell^1 \ell^{1-2\nu}(1+\ell)^2 e^{\theta[1/T(\ell)-1/T(0)]} d\ell, \tag{58}$$

$$I_2(\ell) = \int_\ell^1 \ell^{-1}(1+\ell)^2 \left[e^{\theta[1/T(\ell)-1/T(0)]} - 1\right] d\ell \,. \tag{59}$$

The formulas of Section 3.5, now can be analyzed in detail as the parameters, ν, θ and γ are varied. Variation of ν formally corresponds to changing the reaction order, while a change of θ varies the temperature sensitivity of the reaction. Changing γ corresponds to changing the equation of state, which in turn affects the thermodynamic variables like the temperature. We will give a complete discussion below, but we temporarily turn to the limit of large activation energy.

4.1 Large activation energy

When the activation energy, θ, is large, an analysis of the steady 1-D structure shows that there is a well defined induction zone preceding the main reaction zone. The inverse temperature has the property that its global maximum (temperature minimum) occurs at the shock for $1 < \gamma < 2$. The spatial structure of the detonation wave reflects this property. In the large activation energy limit, if $1 < \gamma < 2$ the spatial structure is an induction zone followed by a relatively thin reaction zone, in which the reaction goes nearly to completion.

For $\gamma > 2$ the temperature at the complete reaction point in the 1-D steady structure is less than the shock temperature. In this case the structure, as measured on the shock-defined induction length scale, consists of an induction-zone, followed by a thin reaction zone, which freezes, i.e. slows exponentially as the temperature decreases below the shock temperature. This has the effect of spreading the reaction zone over exponentially many induction zone lengths.

These statements can be easily understood by simply noticing the profound qualitative effect that changing γ has on the temperature distribution. Figure 1. shows a plot of $T(\ell)$ versus ℓ for varying γ. Note that $\gamma > 2$ *is not* a common range for gas phase detonations. The range *may* have physical significance for condensed phase explosives if it is interpreted as mimicking

the effects of a complex equation of state of a dense fluid and its interaction with endothermic processes which slow the reaction at the end of the reaction zone.

Bdzil, [13], has pointed out that for an ideal caloric equation of state, $(\partial E/\partial \rho)_T \equiv 0$, an ideal thermal equation of state, $P = \rho RT$, and constant specific heats, γ must be restricted to the range $1 < \gamma \leq 5/3$ in order to guarantee a formulation consistent with thermodynamics. Thus, values of $\gamma > 5/3$ should be interpreted with caution.

In the range, $1 < \gamma < 2$, large activation energy asymptotics reduces to finding approximations to (58,59) as $\theta \to \infty$ which is a straightforward exercise in integral asymptotics using Laplace's method. Therefore, the details are not given here. The asymptotic evaluation of (58,59) is completely dominated by the contribution to the integrals near the shock, i.e. at $l = 1$, and one finds to a first approximation that

$$I_1(\ell) \sim I_2(\ell) \sim \frac{e^{\theta(1/T(1)-1/T(0))}}{\theta} \frac{16(\gamma-1)^2}{(3-\gamma)(\gamma+1)^2} \left[1 - e^{\theta \frac{(3-\gamma)(\gamma+1)^2}{4(\gamma-1)^2}(\ell-1)}\right], \quad (60)$$

where

$$1/T(0) - 1/T(1) = \frac{(\gamma+1)^2}{2(\gamma-1)} \frac{\gamma-2}{\gamma}. \quad (61)$$

Even though in $I_2(\ell)$ there is an enhanced contribution near $\ell = 0$, it is still exponentially small in comparison with the contribution to the integral near the shock. To leading order one finds

$$I_1(0) \sim I_2(0) \sim \frac{16(\gamma-1)^2}{(3-\gamma)(\gamma+1)^2} \frac{e^{\theta[1/T(1)-1/T(0)]}}{\theta}. \quad (62)$$

Because of our choice of scales for this paper, the above formulae contain the activation energy scaled with respect to $\tilde{T}_c \equiv \tilde{D}_{CJ}^2/\tilde{R}$. If the one - dimensional steady state shock temperature, $\tilde{T}_s$, had been used instead, (as has been the convention in other studies using activation energy asymptotics), then the shock scaled activation energy,

$$\theta_s = \frac{(\gamma+1)^2}{2(\gamma-1)}\theta \quad (63)$$

would have appeared. Since the main contribution to the integrals is found at the shock, θ_s is the natural large parameter. Especially for values of γ close to one, the value of θ needed to obtain a good asymptotic estimate can be as small as 1. Also it is worth pointing out that in expression (60), the appearance of $\theta(\ell - 1)$ in the argument of the exponential function reflects the existence of the induction zone near the shock.

To illustrate the interpretation of our formulas for the $D_n - \kappa$ relation when the activation energy is large we introduce the induction length scale

$$\tilde{l}_i = \frac{\tilde{D}_{CJ}}{\tilde{k}} \frac{e^{\theta/T(1)}}{\theta} . \tag{64}$$

The relation between the curvature κ scaled with respect to $\tilde{l}_c$ and the curvature κ_i scaled with respect to $\tilde{l}_i$ is

$$\kappa_i = \frac{\tilde{l}_i}{\tilde{l}_c}\kappa = \frac{e^{\theta[1/T(1)-1/T(0)]}}{\theta}\kappa \equiv G(\theta)\kappa. \tag{65}$$

For $\gamma < 2$, $G(\theta)$ is exponentially large as $\theta \to \infty$. Since $I_1(0) \sim I_2(0)$ are proportional to $G(\theta)$, using the above formula with equation (62) in (51) shows that

$$D_n = 1 - \kappa_i A(\gamma) + \kappa_i^{1/\nu} \frac{\nu}{2(1-\nu)} G(\theta)^{-1/\nu} + \ldots, \tag{66}$$

for $0 < \nu \leq 1$ where $A(\gamma) = [16(\gamma - 1)^2]/[(3 - \gamma)(\gamma + 1)^2]$. Notice that the $O(\kappa^{1/\nu})$ term has exponentially small influence in comparison to the $O(\kappa)$ term. One can conclude that for large activation energy effects due to changes in the depletion exponent are not very important in determining the leading order behavior of the $D_n - \kappa$ relation. Since the limit detonation structure for large activation energy is a square wave, our result verifies the leading detonation speed correction to be linear in κ as was anticipated by Wood and Kirkwood, [1].

In the next section we no longer restrict to large activation energy, but consider numerical evaluations of the formulae in Section 3.5.

4.2 Parametric dependence

The effect of curvature and rate state - dependence, according to this paper, has two profound effects, one on detonation velocity and one on the actual structure of the detonation.

The simplest way to illustrate the changes in the detonation velocity with state dependence is to examine how the coefficient $I_1(0)$ changes as ν, γ and θ are varied. The second coefficient $I_2(0)$ essentially follows $I_1(0)$. Figure 2a., shows the variation of $I_1(0)$ with θ for $\nu = 0.5$ fixed and for $\gamma = 1.4, 1.7, 2.0$ and 2.3. The value of $I_1(0)$ is independent of γ for $\theta = 0.0$ since dependence on γ is felt only through the temperature dependence in the integral. For a fixed activation energy, lowering γ towards $\gamma = 1$ increases $I_1(0)$, (corresponding to a $D_n - \kappa$ relation that is more sensitive to changes in the curvature), while increasing γ has the opposite effect. Notice that the activation energy based on the shock temperature is $\theta_s = (\gamma+1)^2/2(\gamma-1) = 7.2\theta$, for $\gamma = 1.4$. So, as $\gamma \to 1$ for fixed θ, the large activation energy results of the last section hold and the *effective* activation energy is large. For fixed γ below a value of approximately 1.7, increasing θ has the effect of increasing $I_1(0)$ and hence the curvature sensitivity. While for γ above this critical value, the curvature dependence is decreased initially with increasing θ, but for θ sufficiently large, the asymptotic dependence of $I_1(0)$ is once again observed and $I_1(0)$ increases with increasing θ according to the asymptotic result. These effects are also seen in other figures discussed below.

Figure 2b. shows the variation of $I_1(0)$ with γ, for fixed activation energies, $\theta = 0.0, 0.5, 1.0$ and 2.0 and fixed depletion exponent, $\nu = 1.0$, and a comparison with the asymptotic result of the last section evaluated with $\theta = 2.0$ is shown. Again for $\theta = 0.0$, $I_1(0)$ is independent of γ, and the figure clearly shows the trends of changing γ mentioned above. For larger values of γ, $I_1(0)$ is less sensitive to changes in θ than for smaller ones and at $\gamma = 1.75$, $I_1(0)$ is essentially independent of θ. This is near the point where $T(1) - T(0)$ changes sign. Importantly, this figure suggests that $\gamma \to 1$ with $\theta \to 0$ is an interesting distinguished limit of the equations of this paper. We have not explored this in detail, to date. The asymptotic comparison appears to be accurate over the entire range of γ evaluated for $\theta = 2.0$, even though the effective value for large θ is decreasing with increasing γ.

Figure 2c. shows the variation of $I_1(0)$ with ν for fixed $\gamma = 1.4$, and

activation energies $\theta = 0, 1.0, 2.0$. The value of $I_1(0)$ appears relatively insensitive to changes in ν until $\nu \to 1$. Recall that when $\nu = 1$ the asymptotic structure of the formulas change and the variation of $I_1(0)$ reflect this. For large values of γ, $I_1(0)$ is less sensitive to changes in θ as is also seen in Figure 2b.

Figures 3a-d show $D_n - \kappa$ curves as various parameters are changed. Figure 3a shows a $D_n - \kappa$ curve for $\gamma = 1.4$, $\theta = 0, .5, 1.0, 2.0$. The curves reflect the exponential sensitivity on the activation energy. Figure 3b. shows similar results except that the value of γ has been changed to 2.0. We find, as mentioned above, that increasing the activation energy, with larger γ, causes the detonation velocity to have a smaller curvature sensitivity, i.e. the trend is reversed from that shown in Figure 3a.. Similar behavior is seen if the activation energy is fixed and γ is decreased towards one. In that case, the reaction zone lengthens exponentially.

In contrast, the sensitivity to changes in ν, for fixed θ is less at smaller γ and greater for larger values of γ. Figure 3c. shows a $D_n - \kappa$ curve for $\gamma = 1.4$, $\theta = 1.0$ with $\nu = 0, 0.3, 0.6, 0.9, 1.0$. The variation between the curves as ν changes is reasonably small, and the logarithmic dependence of $D_n - \kappa$ as $\kappa \to 0$ for $\nu = 1.0$, cannot be seen on the scale of the plot. Figure 3d. shows a similar plot for the same parameters except that $\gamma = 2.0$. The relative variation as ν changes is much greater than that of Figure 3c., and the logarithmic dependence of the $D_n - \kappa$ can be clearly seen for $\nu = 1.0$.

Next we turn to rate state and curvature effects on the detonation structure as computed from our composite expansions. To calculate the spatial dependence of our results, we substituted $u^{(c)}$ for u in equations (52,54) into formula (26) resulting in an integral expression for n which has the accuracy of the composite expansion. Note that the pressure profile and density profile roughly follow that of $u^{(c)}$. The distribution of λ reflects the heat released throughout the structure.

Figure 4a. shows representative plots of λ and $u^{(c)}$, versus n, for $\gamma = 1.4, \nu = 0.5$ and $\theta = 0.0, 0.5, 0.75$ and $\kappa = .02$. The effect of increasing θ is to lengthen the reaction zone. This is generally true for all fixed values of ν and γ. Also, as θ increases from zero, the profiles first develop an inflection point and then concentrate their steepest gradients near the end of the (lengthening) reaction zone. This is coonsistent with the fact that Arrhenius kinetics lead to a square shaped profile in the limit of large activation energy

(Shock - Reaction Zone - Fire).

Figure 4b. shows one of the effects on the structure due to the inclusion of curvature in the structure calculation. The representative spatial structure is calculated for $\gamma = 1.4, \theta = 1.0$ and $\nu = 0.6$ and for values of $\kappa = 0.0$ and .01. The value $\kappa = 0.0$ corresponds to the plane, one - dimensional structure and also the lowest order approximation to the wave structure, while $\kappa = .01$ corresponds to a curved detonation and includes higher order terms. An important feature is the dramatic lengthening of the reaction zone that appears when curvature related terms are retained in the spatial structure of the detonation. This lengthening, all by itself, has important dynamical implication for multi - dimensional numerical simulation.

The numerical rule of thumb for wave propagation problems requires that all dynamically significant features of the flow must be spatially resolved in order to calculate the correct dynamics. In this case we've shown that the rear of the reaction zone, in curved detonation may have an extended tail in which significant heat is released. Proper numerical calculation in a simulation will require resolution of this tail region.

Figure 4c. shows a representative effect of the inclusion of curvature terms on the reaction zone length as ν is varied with $\theta = 1.0, \gamma = 1.4$ and $\kappa = .01$. The variation of the length of the reaction zone, while significant, is not dramatic over the range of values of ν considered. This is in contrast to the qualitative shape of the structure of the reaction zone observed as ν is changed. At low values $\nu < 1/2$, the reaction rate is essentially depletion independent ($\nu = 0.0$) and terminates in a cusp. For higher values of ν an inflection point emerges and a reaction tail involving relatively small rest heat release develops. The transonic layer (TSL) introduced in our matched asymptotic analysis establishes in this tail region (see also [11]). As $\nu \to 1$, the reaction tail extends to infinity. Figure 4d. shows results similar to those of 4c., but with $\gamma = 2.0$ and $\kappa = .05$. Once again the qualitative shape changes with increasing γ. The results in both of these figures can essentially be understood from the one - dimensional structure.

In summary, for the specific case of one step Arrhenius kinetics, we have presented a useful set of approximations for large activation energy which give explicit forms for the $D_n - \kappa$ relation and also can be used to calculate the spatial structure of the reaction zone, essentially analytically. We have evaluated the $D_n - \kappa$ relation's dependence on the parameters of the equation

of state, namely γ, and the kinetics parameters ν and θ. Equation of state parameters, like γ, can mimic the effect of changing kinetics parameters through their influence on the temperature dependence.

At large activation energies, the $D_n - \kappa$ relation is extremely sensitive to changes in the curvature. For fixed, nonzero θ and $\gamma \to 1$, this is also the case. For fixed γ above or below some threshold, increasing and decreasing θ can produce opposite trends in the sensitivity of the $D_n - \kappa$ curve. For very large θ, the reaction zone consists of an induction zone followed by the main reaction layer. The exponential sensitivity, as $\theta \to \infty$, of the D_n-κ relation can be removed by introducing the curvature κ_i scaled with the induction length. Under this scaling, the leading perturbation in terms of κ_i and $1/\theta$ is linear in κ_i. Thus we find, from a systematic analysis, the linear D_n-κ correction that Wood and Kirkwood had anticipated.

In the last three sections we provide the analytical background for the developments in Sections 2.-4. Section 5. introduces Whithams shock ray coordinates, [9], which serve both the description of the detonation shock evolution and a convenient representation of the governing equations.

In Section 6. we derive further results for two dimensions. In particular, we discuss the front evolution equations given a D_n-κ law. We provide a formulation consistent with the ray coordinates and point out the parallel between the present approach for weakly curved detonations and Whitham's Shock Ray Theory.

The goal of Section 7. is to justify the quasi-onedimesional, quasisteady approximations of Sections 2.–4.

5 Front attached coordinates

5.1 The Shock Ray Coordinate System

Here we perform a time dependent transformation from physical space, $(\mathbf{x}, t)$, to the variables $(\xi, \underline{\zeta}, \tau)$, where

$$\xi \qquad \text{and} \qquad \underline{\zeta} = (\zeta^1, \zeta^2) \tag{67}$$

are spatial coordinates to be defined shortly and

$$\tau \equiv t \ . \tag{68}$$

In analogy to Huyghens' principle, orthogonal trajectories of successive shock surfaces, called the 'shock rays', serve as coordinate lines of the normal coordinate, ξ. With each point $\mathbf{x}$ on a shock ray, one associates a unit normal vector, $\mathbf{n}(\mathbf{x})$, and a scalar wave speed, $\hat{D}(\mathbf{x})$, follows: $\mathbf{n}(\mathbf{x})$ is the unit tangent to the shock ray at $\mathbf{x}$ and $\hat{D}(\mathbf{x})$ is the value of the front normal velocity, D_n, in $\mathbf{x}$ at the instant when the detonation shock passes the point.

Let $\mathbf{x} = \mathbf{x}_0(\underline{\zeta})$ parametrize the initial shock surface, then ζ^i $(i = 1,2)$ label the shock rays emanating from this reference front, so that

$$\underline{\zeta} = \text{const} \qquad \text{along shock rays.} \tag{69}$$

We specify the normal coordinate ξ by:

i) At any given time, τ, the arclength, ds, of a line element on a shock ray at a point $\mathbf{x}$ is given by

$$ds = \hat{D}(\mathbf{x})\, d\xi \ . \tag{70}$$

ii) A point $\mathbf{x}(\xi, \underline{\zeta}, \tau)$ with $(\xi, \underline{\zeta}) = \text{const}$ moves in time along a ray at the speed $\hat{D}$, i.e.,

$$ds = \hat{D}(\mathbf{x})\, d\tau \ . \tag{71}$$

iii) $\xi \equiv 0$ on the detonation shock.

It follows from *i)* and *ii)* that

$$\frac{\partial \mathbf{x}}{\partial \xi}(\xi, \underline{\zeta}, \tau) = \frac{\partial \mathbf{x}}{\partial \tau}(\xi, \underline{\zeta}, \tau) = (\hat{D}\mathbf{n})(\mathbf{x}(\xi, \underline{\zeta}, \tau)) \ , \tag{72}$$

and that all metric functions associated with the coordinate transformation will depend only on the combination of variables $(\underline{\zeta}, \xi + \tau)$. For example, $\mathbf{x}(\xi, \underline{\zeta}, \tau) = \mathbf{x}(\underline{\zeta}, \xi + \tau)$, $\mathbf{n}(\xi, \underline{\zeta}, \tau) = \mathbf{n}(\underline{\zeta}, \xi + \tau)$ etc. In particular, $\hat{D}(0, \underline{\zeta}, \tau) \equiv D_n(\underline{\zeta}, \tau)$ is the actual detonation shock speed at time τ. The ζ^i $(i = 1,2)$ are a set of tangential coordinates in the surfaces $\xi = \text{const}$.

5.2 The metric

(For the differential geometry used below, the reader may confer Struik [14] and Millman and Parker [15].)

In the following, we let upper and lower roman indices cover the range $\{1,2\}$, while greek indices cover $\{0,1,2\}$ and we use the summation convention for the respective ranges of the indices. For convenience, we define

$$\zeta^0 \equiv \xi \,. \tag{73}$$

The vectors

$$\mathbf{g}_0 = \frac{\partial \mathbf{x}}{\partial \xi} \equiv (\hat{D}\,\mathbf{n})(\underline{\zeta}, \xi + \tau) \qquad \text{and} \qquad \mathbf{g}_i = \frac{\partial \mathbf{x}}{\partial \zeta^i}(\underline{\zeta}, \xi + \tau) \tag{74}$$

form the local covariant basis, $\{\mathbf{g}_0, \mathbf{g}_1, \mathbf{g}_2\}$, associated with the mapping $(\xi, \underline{\zeta}) \rightarrow \mathbf{x}$. The covariant basis determines the covariant metric coefficients,

$$(g_{\nu\mu}) = (\mathbf{g}_\nu \cdot \mathbf{g}_\mu) = \begin{pmatrix} \hat{D}^2 & 0 \\ 0 & g_{ij} \end{pmatrix} . \tag{75}$$

The yet unknown coefficients (g_{ij}), $(i,j = 1,2)$ characterize the transverse parametrization. The zeroes in (75) arise because the rays are orthogonal trajectories of the shock surfaces so that $(\mathbf{g}_0 \sim \mathbf{n} \perp \mathbf{g}_i)$.

Associated with the covariant basis, $\{\mathbf{g}_\nu\}$, is its dual, $\{\mathbf{g}^\nu\}$, the contravariant basis. It is defined by

$$\mathbf{g}^\mu \cdot \mathbf{g}_\nu = \delta^\mu{}_\nu \,, \tag{76}$$

where $\delta^\mu{}_\nu$ is the Kronecker Delta. An alternative but equivalent definition of the contravariant basis is given by

$$\mathbf{g}^0 = \mathrm{grad}(\xi) = (\frac{1}{\hat{D}}\,\mathbf{n})(\underline{\zeta}, \xi + \tau) \qquad \text{and} \qquad \mathbf{g}^i = \mathrm{grad}(\zeta^i) \,. \tag{77}$$

The reader may verify that (74), (76), and (77) are consistent. For later reference, we notice that the Jacobian determinant of the coordinate mapping is,

$$J = \mathbf{g}_0 \cdot (\mathbf{g}_1 \times \mathbf{g}_2) = \sqrt{\det(g_{\nu\mu})} = \hat{D}\,\hat{A} \,, \qquad \text{with} \qquad \hat{A} = \sqrt{\det(g_{ij})} \,. \tag{78}$$

The Jacobian relates volume elements in physical space to volume elements in the coordinate space through $dV = J\ d\xi\ d\zeta^1\ d\zeta^2$. The physical meaning of $\hat{A}$ as a ray tube area function will become clear later in Section 6.

5.3 The velocity field

The velocity relative to the moving coordinate frame, i.e., relative to a point $(\xi, \zeta) = \text{const}$ is

$$\mathbf{v} = v^\nu\, \mathbf{g}_\nu = u\mathbf{n} + v^i\, \mathbf{g}_i\ , \tag{79}$$

where the $\{v^\nu\}$ are the contravariant velocity components. Notice, that $v^0 = u/\hat{D}$ is the contravariant normal velocity coordinate, while u is the *physical value* of normal velocity relative to the shock attached reference frame. Recalling (72), we write the velocity in an inertial frame as

$$\mathbf{v}^{\text{lab}} = (u + \hat{D})\,\mathbf{n} + v^i\, \mathbf{g}_i\ . \tag{80}$$

5.4 The transformed governing equations

The reactive Euler equations which govern the detonation phenomena are:

$$\begin{aligned}
\frac{\mathcal{D}\rho}{\mathcal{D}\tau} + \rho\,\text{div}(\mathbf{v}^{\text{lab}}) &= 0 \\
\frac{\mathcal{D}\mathbf{v}^{\text{lab}}}{\mathcal{D}\tau} + \frac{1}{\rho}\text{grad}(P) &= 0 \\
\frac{\mathcal{D}E}{\mathcal{D}\tau} - \frac{p}{\rho^2}\frac{\mathcal{D}\rho}{\mathcal{D}\tau} &= 0 \\
\frac{\mathcal{D}\lambda}{\mathcal{D}\tau} &= r\ .
\end{aligned} \tag{81}$$

The previous subsection defined the nomenclature needed to express the differential operators in these equations in terms of the new coordinates. Here we summarize the results of these transformations. Some relations that are special to our particular choice of coordinates are derived in appendix(A).

The gradient operator reads

$$\text{grad} = \mathbf{g}^{\nu}\frac{\partial}{\partial\zeta^{\nu}} = \frac{1}{\hat{D}}\mathbf{n}\frac{\partial}{\partial\xi} + \mathbf{g}^{i}\frac{\partial}{\partial\zeta^{i}} \tag{82}$$

as a consequence of (77). The particle time derivative (App. A.1) is

$$\frac{\mathcal{D}}{\mathcal{D}\tau} = \frac{\partial}{\partial\tau} + \frac{u}{\hat{D}}\frac{\partial}{\partial\xi} + v^{i}\frac{\partial}{\partial\zeta^{i}} \; . \tag{83}$$

Applied to the velocity in an inertial frame, $\mathbf{v}^{\text{lab}}$ in (80), this operator yields the acceleration

$$\begin{aligned}\frac{\mathcal{D}\mathbf{v}^{\text{lab}}}{\mathcal{D}\tau} &= \mathbf{n}\frac{\mathcal{D}}{\mathcal{D}\tau}(u+\hat{D}) + \mathbf{g}_i\frac{\mathcal{D}v^{i}}{\mathcal{D}\tau} + \\ &+ (u+\hat{D})\left[(1+\frac{u}{\hat{D}})\frac{\partial\mathbf{n}}{\partial\xi} + v^{j}\frac{\partial\mathbf{n}}{\partial\zeta^{j}}\right] \\ &+ v^{i}\left[(1+\frac{u}{\hat{D}})\frac{\partial\mathbf{g}_i}{\partial\xi} + v^{j}\frac{\partial\mathbf{g}_i}{\partial\zeta^{j}}\right] .\end{aligned} \tag{84}$$

The derivation uses the fact mentioned below (72) that the metric functions depend on (ξ,τ) only via $(\xi+\tau)$.
The flow divergence, as derived in appendix A.2, is

$$\text{div}(\mathbf{v}^{\text{lab}}) = \frac{1}{\hat{D}}\frac{\partial}{\partial\xi}(u+\hat{D}) + \kappa\,(u+\hat{D}) + \frac{1}{J}\frac{\partial}{\partial\zeta^{i}}(Jv^{i}) \; . \tag{85}$$

Using (82)–(85), we rewrite the governing equations, thereby collecting on the right hand sides all terms that have been neglected in (2) – (5).

The mass conservation equation, $(81)_1$, becomes

$$\frac{u}{\hat{D}}\frac{\partial\rho}{\partial\xi} + \frac{\rho}{\hat{D}}\frac{\partial}{\partial\xi}(u+\hat{D}) + \rho\kappa\,(u+\hat{D}) = -\left(\frac{\partial\rho}{\partial\tau} + v^{i}\frac{\partial\rho}{\partial\zeta^{i}} + \frac{\rho}{J}\frac{\partial}{\partial\zeta^{i}}(Jv^{i})\right) \; . \tag{86}$$

The momentum equation, $(81)_2$, reads

$$\frac{\mathcal{D}\mathbf{v}^{\text{lab}}}{\mathcal{D}\tau} = -\frac{1}{\rho}\text{grad}(P) \tag{87}$$

with the left hand side from (84) and the gradient evaluated according to (82). Of interest for our discussion are the normal and tangential components of

this vector equation. Scalar multiplication by $\mathbf{n}$ and $\mathbf{g}^i$ and some algebra using (144) in App. B.1 and the orthogonality of $\mathbf{n}$ and the $\{\mathbf{g}_i\}$ yields

$$\frac{\mathcal{D}}{\mathcal{D}\tau}(u+\hat{D})+\frac{1}{\rho\hat{D}}\frac{\partial P}{\partial \xi}=-\left(1+\frac{u}{\hat{D}}\right)v^i\frac{\partial \hat{D}}{\partial \zeta^i}+v^iv^j\mathbf{g}_j\cdot\frac{\partial \mathbf{n}}{\partial \zeta^i} \tag{88}$$

and

$$\begin{aligned}\frac{\mathcal{D}v^j}{\mathcal{D}\tau} &+ 2\left(u+\hat{D}\right)v^i\mathbf{g}^j\cdot\frac{\partial \mathbf{n}}{\partial \zeta^i}+v^iv^k\mathbf{g}^j\cdot\frac{\partial \mathbf{g}_i}{\partial \zeta^k}\\ &= -\frac{1}{\rho}g^{ij}\frac{\partial P}{\partial \zeta^i}+\frac{(u+\hat{D})^2}{\hat{D}}g^{ij}\frac{\partial \hat{D}}{\partial \zeta^i}\,.\end{aligned} \tag{89}$$

In sections 2.–4. we are interested only in first order approximations and do not need to solve the transverse momentum equation. We go back to (89) only in section 6.2 below where we analyse the two-dimensional case and obtain estimates for the tangential velocities, v^i. These are needed to justify the quasi-onedimensional, quasisteady approximation in sections 2.–4.

The energy and reaction progress equations, (81)c,d, are written solely in terms of particle time derivatives and thus remain unchanged under the transformation. With the understanding that $\mathcal{D}/\mathcal{D}\tau$ is the operator in (83) we obtain

$$\frac{u}{\hat{D}}\frac{\partial E}{\partial \xi}-\frac{P}{\rho^2}\frac{u}{\hat{D}}\frac{\partial \rho}{\partial \xi}=-\Big(\frac{\partial E}{\partial \tau}+v^i\frac{\partial E}{\partial \zeta^i}-\frac{P}{\rho^2}\Big[\frac{\partial \rho}{\partial \tau}+v^i\frac{\partial \rho}{\partial \zeta^i}\Big]\Big)\,, \tag{90}$$

$$\frac{u}{\hat{D}}\frac{\partial \lambda}{\partial \xi}-r\,(p,\rho,\lambda)=-\Big(\frac{\partial \lambda}{\partial \tau}+v^i\frac{\partial \lambda}{\partial \zeta^i}\Big)\,. \tag{91}$$

Sections 2.–4. focus on asymptotic solutions to the Master equation, (15). One obtains a generalized version of this equation from the energy equation by replacing

$$\frac{\mathcal{D}E}{\mathcal{D}\tau}(p,\rho,\lambda)=E_P\frac{\mathcal{D}P}{\mathcal{D}\tau}+E_\rho\frac{\mathcal{D}\rho}{\mathcal{D}\tau}+E_\lambda\frac{\mathcal{D}\lambda}{\mathcal{D}\tau} \tag{92}$$

and inserting appropriate expressions for $\mathcal{D}(P,\rho,\lambda)/\mathcal{D}\tau$ using the mass, normal momentum and reaction progress equations. The result is

$$(c^2 - u^2)\frac{1}{\hat{D}}\frac{\partial u}{\partial \xi} + \left[\kappa c^2(u + \hat{D}) - c^2\sigma r\right] = \text{h.o.t.} \tag{93}$$

where h.o.t. abbreviates all terms that are neglected in (15). Its precise form is:

$$\begin{aligned} \text{h.o.t.} \;=\; & u\frac{\partial u}{\partial \tau} - \frac{1}{\rho}\frac{\partial P}{\partial \tau} - \frac{c^2}{J}\frac{\partial}{\partial \zeta^i}(J\, v^i) \\ & - (c^2 - u^2 - u\hat{D})\frac{1}{\hat{D}}\frac{\partial \hat{D}}{\partial \tau} + \frac{1}{2}v^j\frac{\partial u^2}{\partial \zeta^j} + \frac{\mathcal{D}\mathrm{v}_{||}^2}{\mathcal{D}\tau} \\ & + uv^i\frac{\partial \hat{D}}{\partial \zeta^i} + \hat{D}\mathrm{v}_{||}\cdot\frac{\mathcal{D}\mathrm{n}}{\mathcal{D}\tau}\,, \end{aligned} \tag{94}$$

where $\mathrm{v}_{||} = v^i\mathbf{g}_i$ is the velocity component in the tangential direction and

$$c^2\sigma = \frac{-E_\lambda}{\rho E_p} = \frac{1}{2(\gamma+1)}\,. \tag{95}$$

The speed of sound appears in the derivation through the expression $c^2 = -(E_\rho - p/\rho^2)/E_p$.

6 Front evolution in two dimensions

Here we are interested in the overall evolution of the detonation surface, but not in resolving the structure of the thin reaction zone. The appropriate scaled coordinates measuring on the length scale of a typical radius of curvature are

$$(\hat{\xi}, \hat{\zeta}, \hat{\tau}) = \delta\,(\xi, \zeta^1, \tau)\,, \tag{96}$$

where δ is a typical value of the nondimensional curvature, i.e.,

$$\hat{\kappa} = \frac{1}{\delta}\kappa = O(1) \qquad \text{as} \qquad \delta \to 0\,. \tag{97}$$

In two dimensions, the co and contravariant bases reduce to

$$\{\mathbf{g}_0, \mathbf{g}_1\} = \{\hat{D}\,\mathbf{n}, \hat{A}\,\mathbf{t}\} \qquad \text{and} \qquad \{\mathbf{g}^0, \mathbf{g}^1\} = \{\frac{1}{\hat{D}}\,\mathbf{n}, \frac{1}{\hat{A}}\,\mathbf{t}\}\ , \tag{98}$$

where $\mathbf{t}$ is a unit tangent vector pointing towards increasing $\hat{\zeta}$. The length, $\hat{A}$, of $\mathbf{g}_1$ determines an arclength increment along a surface $\xi = \text{const}$ via

$$d\hat{s} = \hat{A}\, d\hat{\zeta}\ . \tag{99}$$

The two functions $(\hat{D}, \hat{A})(\hat{\zeta}, \hat{\xi} + \hat{\tau})$ completely describe the metric of the ray coordinate system. We note that $\hat{D}$ corresponds to Whitham's Mach number, M, while $\hat{A}$ is his ray tube "area function".

Basic differential geometric calculations using (98) and (137), (142) in appendix A.2 show that $\hat{A}$ evolves along a shock ray according to

$$\frac{1}{\hat{A}\hat{D}}\frac{\partial \hat{A}}{\partial \hat{\xi}} = \hat{\kappa} \tag{100}$$

(see also Whitham's eq.(8.48), [9].) This relation is also valid in three dimensions provided $\hat{A}$ is defined by (78)b.

6.1 Whitham's approach for inert shocks

The normal $\mathbf{n}$ is, in two dimensions, uniquely defined by the angle θ with respect to a fixed reference line, say the x-axis of a Cartesian frame, i.e.,

$$\mathbf{n} = \cos\theta\,\mathbf{i} + \sin\theta\,\mathbf{j}\ . \tag{101}$$

The relation for changes of $\mathbf{n}$ along the shock line becomes

$$\mathbf{t}\cdot\frac{1}{\hat{A}}\frac{\partial \mathbf{n}}{\partial \hat{\zeta}} = \hat{\kappa} = -\frac{\partial \theta}{\partial \tilde{s}} = -\frac{1}{\hat{A}}\frac{\partial \theta}{\partial \hat{\zeta}}\ , \tag{102}$$

and we find

$$\frac{\partial \theta}{\partial \hat{\zeta}} = -\frac{1}{\hat{D}}\frac{\partial \hat{A}}{\partial \hat{\xi}} \tag{103}$$

from (100). On the other hand, θ is also the angle of $\mathbf{t}$ with respect to the y-axis and from symmetry considerations regarding the respective roles of $(\hat{\xi}, \hat{D})$ and $(\hat{\zeta}, \hat{A})$ one concludes that

$$\frac{\partial\theta}{\partial\hat{\xi}} = \frac{1}{\hat{A}}\frac{\partial\hat{D}}{\partial\hat{\zeta}} \,. \tag{104}$$

Whitham derives a differential equation relating the area function $\hat{A}$ and the front velocity $\hat{D}$ from his semi-heuristic characteristic rule:

$$G(\hat{D})\frac{\partial\hat{D}}{\partial\hat{\xi}} + \frac{1}{\hat{A}}\frac{\partial\hat{A}}{\partial\hat{\xi}} = 0 \,. \tag{105}$$

With $G(\hat{D})$ a known function, this equation integrates to a relation $\hat{A} = \hat{A}(\hat{D})$ if the initial parametrization is chosen such that $\hat{A}(\hat{\zeta}, 0) \equiv 1$. Inserting this in (103) and (104) yields a hyperbolic 2×2-sytem of equations for θ and $\hat{D}$, which intrinsically, i.e., without reference to the flowfield, describes the shock evolution.

6.2 Detonation Shocks

Consider now the asymptotic weak curvature detonation theory. Instead of an "area rule" $\hat{A} = \hat{A}(\hat{D})$, we have a coupling $\hat{D} = \hat{D}(\hat{\kappa})$. Choosing $\hat{\kappa}$ as a basic dependent variable and eliminating $\hat{D}$, (see App. B.1), we obtain

$$\frac{\partial\hat{\kappa}}{\partial\hat{\xi}} = -\left[\hat{\kappa}^2\hat{D}(\hat{\kappa}) + \left(\frac{1}{\hat{A}}\frac{\partial}{\partial\hat{\zeta}}\right)^2 \hat{D}(\hat{\kappa})\right] . \tag{106}$$

Together with (100) this relation forms the desired system of equations for the evolution of the metric functions $\hat{\kappa}, \hat{A}$ on the $\hat{\tau}$ time scale. An equivalent equation was derived in [5]. Recall that the detonation speed–curvature relations derived in sections 2.–4. may be written as

$$\hat{D}(\hat{\kappa}) = 1 - \delta^* D^*(\hat{\kappa}, \delta) + o([\delta^*]^2) \tag{107}$$

for all $0 < \nu \leq 1$, if we define

$$\delta^* = \begin{cases} \delta & \text{for} \quad \nu < 1 \\ \delta \ln(1/\delta) & \text{for} \quad \nu = 1 \end{cases} . \tag{108}$$

Here, we require that

$$D^*(\hat{\kappa},\delta) = O(1) \qquad \text{as} \qquad (\delta \to 0)\ , \tag{109}$$

but allow for an explicit dependence on δ of D^* to account for the two-gauge function expansions in (43) and (49) for D_n'.

With $\hat{D} - 1 = O(\delta^*) \ll 1$, the second derivative in (106) is negligble unless the typical tangential length scale is small. Tangential variations of the front geometry play a significant role in the curvature equation only if they depend explicitly on the stretched tangential variable

$$z = \frac{1}{\sqrt{\delta^*}}\hat{\zeta} = \frac{\delta}{\sqrt{\delta^*}}\zeta\ . \tag{110}$$

In that case, $(\hat{\kappa}, \hat{A})$ obey

$$\begin{aligned} \frac{\partial \hat{A}}{\partial \hat{\xi}} &= \hat{\kappa}\hat{A}\hat{D} \\ \frac{\partial \hat{\kappa}}{\partial \hat{\xi}} &= -\hat{\kappa}^2\hat{D} + \frac{1}{\hat{A}}\frac{\partial}{\partial z}\left(\frac{1}{\hat{A}}\frac{\partial}{\partial z}D^*(\hat{\kappa},\delta)\right) \end{aligned} \tag{111}$$

to leading order. This system replaces Whithams equations in the theory for weakly curved diverging detonations.

It was also found earlier by Bdzil and Stewart, [16], in a different approach, that the D-κ relation of the asymptotic theory leads to a *parabolic* behavior of the surface dynamics. This is in contrast with Whitham's *hyperbolic* shock dynamics model.

Given smooth initial data for $(\hat{A}, \hat{\kappa})$ the system (111) describes the evolution of the shock geometry on the $\hat{\tau}$-time scale. Since the present asymptotic theory is restricted to diverging waves with $\hat{\kappa} > 0$, [11], the area function, $\hat{A}$, will continously increase, thereby diminishing the influence of the diffusive term in (111)b. Asymptotically, this leads to $\hat{D} \approx 1$, $\partial\hat{A}/\partial\hat{\xi} \approx \hat{\kappa}\hat{A}$ and $\partial\hat{\kappa}/\partial\hat{\tau} = -\hat{\kappa}^2$ for the curvature at $\xi = 0$. This system is equivalent to Huyghens' principle which predicts smooth solutions for all times for diverging waves. Thus, we expect solutions to (111) to be smooth as well, although the nonlinearity in the diffusion-like term, induced by $D^* = D^*(\hat{\kappa},\delta)$ might deserve a detailed analysis for particular functions $D^*(\cdot,\cdot)$.

As long as the solutions are smooth in the $(z, \hat{\tau})$–variables we can assess the order of magnitude of the metric terms in (86)–(93) needed for a justification of the reduced equations. This will be one topic of section 7.

7 Justification of the simplified asymptotic equations

To acchieve the goal of this section, we go back to the transformed governing equations of section 5. We assess the metric functions, such as $(1/J)\partial J/\partial\zeta^i$ or $\mathbf{g}^j \cdot \partial \mathbf{n}/\partial\zeta^j$, the tangential velocities, $\{v^i\}$, and their tangential derivatives. From this we derive a posteriori estimates for the accuracy of our approximations, that is, given the results of sections 2.–4. and the front propagation law, we show that the neglected terms all contribute to higher than first order in a small curvature expansion.

7.1 An estimate for the transverse velocities

The estimate of the tangential velocity component, v^1, uses a transformation of the tangential momentum balance. Using the two-dimensional result $(1/\hat{A})\partial \mathbf{n}/\partial\hat{\zeta} = \hat{\kappa}\,\mathbf{t}$, (98) and (102) the metric terms in the tangential momentum balance (89) become

$$v^i \mathbf{g}^j \cdot \frac{\partial \mathbf{n}}{\partial \hat{\zeta}^i} = v^1 \hat{\kappa} \qquad \text{and} \qquad v^i v^k \mathbf{g}^j \cdot \frac{\partial \mathbf{g}_i}{\partial \hat{\zeta}^k} = (v^1)^2 \frac{1}{\hat{A}} \frac{\partial \hat{A}}{\partial \hat{\zeta}} \,. \tag{112}$$

For convenience, we recall (100), namely $\partial \hat{A}/\partial\hat{\xi} = \hat{\kappa}\hat{A}\hat{D}$. Then, by multiplying (89) with $\hat{A}$ and adding,

$$v^1 \frac{\mathcal{D}\hat{A}}{\mathcal{D}\hat{\tau}} = (\hat{A}\, v^1) \left(\hat{\kappa}\,(u + \hat{D}) + v^1 \frac{1}{\hat{A}} \frac{\partial \hat{A}}{\partial \hat{\zeta}} \right) \tag{113}$$

to the left-hand and right-hand sides, respectively, we arrive at

$$\frac{\mathcal{D}}{\mathcal{D}\hat{\tau}}(\hat{A}\, v^1) + \hat{\kappa}\,(u + \hat{D})(\hat{A}\, v^1) = -\frac{1}{\rho \hat{A}} \frac{\partial P}{\partial \hat{\zeta}} + \frac{(u + \hat{D})^2}{\hat{D}} \frac{1}{\hat{A}} \frac{\partial \hat{D}}{\partial \hat{\zeta}} \,. \tag{114}$$

Given the solutions $(\hat{\kappa}, \hat{A})$ and (P, ρ, u) to the wave propagation problem in section 6.1 and to the detonation structure problem in sections 2.-4., respectively, this is an ordinary differential equation for $(\hat{A}\, v^1)$ along a particle path. The exact solution, taking into account that $v^1 \equiv 0$ at the shock, is

$$(\hat{A}\, v^1) = e^{-\Phi} \; {}^{pp}\!\int_0^{\hat{\tau}} e^{\Phi} \left[-\frac{1}{\rho \hat{A}} \frac{\partial P}{\partial \hat{\zeta}} + \frac{(u + \hat{D})^2}{\hat{D}} \frac{1}{\hat{A}} \frac{\partial \hat{D}}{\partial \hat{\zeta}^1} \right] d\hat{\tau}' \,, \tag{115}$$

where

$$\Phi = {}^{pp}\!\int_0^{\hat{\tau}} \hat{\kappa}(u + \hat{D})\, d\hat{\tau}' \,, \tag{116}$$

and ${}^{pp}\!\int$ denotes integration along a particle path. Next we observe that $(\hat{A}, \hat{D}) \approx$ const within MRL and TSL to order $O(\delta^*)$, because $(\hat{A}, \hat{D})$depend on $\hat{\xi}$ only through the combination $\hat{\xi} + \hat{\tau}$, and the thickness of the layers in terms of $\hat{\xi}$ is no larger than $O(\delta^*)$ as $(\delta \to 0)$. Using the quasisteady composite solutions for the detonation structure in section 3.5 one can derive an explicit representation for $(\hat{A}\, v^1)$ valid throughout the subsonic region of the detonation structure. However, here we are mainly interested in an order of magnitude estimate:

Observing that (i) the thickness of the subsonic region is of order $O(\delta^*)$, that (ii) particles pass by at an order $O(1)$ velocity, that (iii) the strongest transverse pressure gradients occur in the transonic layer for $\nu = 1$,

$$\frac{\partial P}{\partial \hat{\zeta}} = O\left(\frac{\delta^{1/2}}{(\delta^*)^{1/2}} \frac{\partial P^{(1/2)}}{\partial z} \right) = O\left(\frac{1}{\ln^{1/2}(1/\delta)} \right) \tag{117}$$

and that (iv)

$$\frac{\partial \hat{D}}{\partial \hat{\zeta}} = -\frac{\delta^*}{\sqrt{\delta^*}} \frac{\partial D^*}{\partial z} + \cdots = O([\delta \ln(1/\delta)]^{1/2}) \,, \tag{118}$$

we find that the solution in (115) yields

$$(\hat{A}\, v^1) = O((\delta \delta^*)^{1/2}) = O((\delta \ln^{1/2}(1/\delta)) \qquad \text{for} \qquad (\nu = 1) \,. \tag{119}$$

For $\nu < 1$ the estimate is even stronger, namely $(\hat{A}\, v^1) = O(\delta^{\frac{1}{2}[\frac{1}{\nu}+1]})$.

7.2 Error terms in the governing equations

In this section, we compare the terms neglected with the smallest terms kept from the transformed governing equations (86)–(93). The estimates assume that the matched asymptotic solutions are of the following form when written in terms of the variables $(\xi, \underline{\zeta}, \tau)$:

$$f(\xi, \underline{\zeta}, \tau) = f^{(0)}(\xi) + \delta^* f^*(\xi, \underline{z}, \hat{\tau}; \delta) + O([\delta^*]^2) \qquad \text{in MRL} \tag{120}$$

and

$$f(\xi, \underline{\zeta}, \tau) = f_{\text{CJ}} + \delta^{1/2\nu} f^{(1/2\nu)}(\delta^{-\alpha}\xi, \underline{z}, \hat{\tau}) + O(\delta^*) \qquad \text{in TSL.} \tag{121}$$

Here f stands for (p, ρ, u) and $\alpha = 1/\nu - 1$ for $\nu \leq 1$ and we use the notation for δ^* as in (107).

We recall that the solutions were originally obtained in terms of the reaction progress variables $\ell = \sqrt{1-\lambda}$ and $s = \kappa^{-1/\nu}(1-\lambda)$, respectively. Since, in general, $\lambda = \lambda(\xi, \underline{\zeta}, \tau)$, it is not trivial that the representations in (120) and (121) are valid. They imply that the reaction progress equation is solved to first order accuracy by the inverse solutions

$$\xi = \xi^{(0)}(\ell) + \delta^* \xi^*(\ell, \underline{z}, \hat{\tau}; \delta) + O([\delta^*]^2) \qquad \text{in MRL} \tag{122}$$

and

$$\xi = \xi_b + \delta^\alpha \xi^*_{\text{TSL}}(s, \underline{z}, \hat{\tau}; \delta) + o(\delta^\alpha) \qquad \text{in TSL.} \tag{123}$$

Given the results of sections 2.–4., one can construct such solutions a posteriori by straight-forward but tedious calculations.

We emphasize that $\xi = \xi^{(0)}(\ell)$ being independent of $\underline{z}, \tau$ requires that the reaction rate is not extremely sensitive in the sense of a distinguished limit of the curvature and the sensitivity parameter of the rate function. For example, with an Arrhenius reaction rate, as considered in section 4., a limit $\kappa_i \theta_s = O(1)$ as $\kappa_i \to 0$ for curvature and activation energy is excluded. (see (65) for the definition of κ_i.) In such a regime, the main reaction layer thickness changes by order $O(1)$ due to the curvature induced perturbations and the appropriate Ansatz for ξ is $\xi = \xi^{(0)}(\ell, \kappa(\underline{z}, \tau))$. Buckmaster [18] studies a

curvature-activation energy limit for overdriven waves. He points out that the reaction zone structure remains quasisteady if the long time variable, $\bar{\tau}$, is the only relevant time variable in the process, but that, for sufficiently short tangential characteristic lengths, the changes of the induction zone thickness induce transverse waves in the burnt gases. This is an inherently unsteady effect and is not accounted for in the present analysis. In particular, the discussion following (110) would have to be revised. Notice, however, that these restrictions do not prevent us from considering the *sequential* limit ($\kappa_i \to 0$) *then* $\theta_s \to \infty$ of section 4.

From here on, we assume the form of the solutions in (120)–(121) and go back to the transformed governing equations. The terms including metric functions are assessed in the framework of section 6.1, so that

$$\begin{aligned} \hat{D} &= 1 - \delta^* D^*(z, \hat{\tau}; \delta) + O([\delta^*]^2) \\ \hat{A} &= \hat{A}^{(0)}(z, \hat{\tau}; \delta) + O(\delta^*) \\ \hat{\kappa} &= \hat{\kappa}^{(0)}(z, \hat{\tau}; \delta) + O(\delta^*) \ . \end{aligned} \tag{124}$$

and

$$J = \hat{A}\hat{D} = \hat{A}^{(0)} + \delta^*(\hat{A}^* - D^*\hat{A}^{(0)}) + \cdots \ , \tag{125}$$

with z, δ^* from (110) and (107), respectively. Again, the explicit δ - dependences indicate that the functions contain the leading terms for two-gauge function expansions in δ.

Using the definitions for $(\hat{\xi}, \hat{\zeta}, \hat{\tau})$ in (96), the equations (98) for the co- and contravariant bases, (102) and the estimate (119) for $v^{(1)}$, we obtain

$$\frac{1}{J}\frac{\partial}{\partial \zeta^j}(Jv^i) = O(\delta^{3/2}) \tag{126}$$

for the neglected term in (86) and

$$v^i \left(1 + \frac{u}{\hat{D}}\right) \frac{\partial \hat{D}}{\partial \zeta^i} = O(\delta^{3/2}\delta^*) \qquad \text{and} \qquad v^i v^j \mathbf{g}_j \cdot \frac{\partial \mathbf{n}}{\partial \zeta^i} = O(\delta^2 \delta^*) \tag{127}$$

for the metric functions in (88).

The Ansätze in (120) and (121), and again (119) yield for $f = (p, \rho, u)$:

$$\frac{\partial f}{\partial \tau} + v^i \frac{\partial f}{\partial \zeta^i} = O(\delta\delta^*, \delta^{3/2}\delta^*) \qquad \text{in MRL} . \tag{128}$$

and

$$\frac{\partial f}{\partial \tau} + v^i \frac{\partial f}{\partial \zeta^i} = O(\delta^{1+\frac{1}{2\nu}}, \delta^{\frac{3}{2}+\frac{1}{2\nu}}) \qquad \text{in TSL} . \tag{129}$$

On the other hand, the smallest terms kept from the continuity equation are of the order

$$\rho\kappa(u + \hat{D}) = O(\delta) \tag{130}$$

in both layers, which is large compared to (126) and (128). The smallest terms kept from the energy and normal momentum equations are of the form

$$\delta^{1/\nu} u^{(0)} \frac{\partial f^{(1/\nu)}}{\partial \xi} = O(\delta^{1/\nu}) \qquad \text{for} \qquad (\nu \leq 1) \qquad \text{in MRL} \tag{131}$$

and

$$\delta^{1-\frac{1}{2\nu}} u_{\mathrm{CJ}} \frac{\partial f^{(1/2\nu)}}{\partial \xi_{\mathrm{TSL}}} = O(\delta^{1-\frac{1}{2\nu}}) \qquad \text{for} \qquad (\nu \leq 1) \qquad \text{in TSL} \tag{132}$$

Here we used $\xi_{\mathrm{TSL}} = \delta^{-\alpha}(\xi - \xi_b)$ with $\alpha = 1/\nu - 1$ from (121). Comparison with (128) and (129), respectively, shows that the quasisteady, quasi-onedimensional equations are a consistent leading order approximation in the present regime. We finally obtain (2)–(5) by (i) replacing ξ with the shock ray arclength coordinate n on a ray satisfying $dn = \hat{D}d\xi$ and (ii) using the fact that the variation of $\hat{D}$ through the layers is of order δ^* only, thus setting it to its value, D_n, at the detonation shock.

A Differential Operators

A.1 Particle Time Derivative

Beginning with a formulation in terms of cartesian coordinates $(t, x^\nu), (\nu = 0, 1, 2)$, we write

$$\frac{\mathcal{D}}{\mathcal{D}t} = \frac{\partial}{\partial t}\bigg|_{\mathbf{x}} + \mathbf{v}^{\text{lab}} \cdot \text{grad}(\ ) \ . \tag{133}$$

The coordinate transformation, $(t, x^\nu) \to (\tau, \zeta^\nu)$, implies

$$\frac{\partial}{\partial \tau} = \frac{\partial}{\partial t}\bigg|_{\mathbf{x}} + \frac{\partial \mathbf{x}}{\partial \tau} \cdot \text{grad}(\ ) \ , \tag{134}$$

such that

$$\frac{\mathcal{D}}{\mathcal{D}t} = \frac{\partial}{\partial \tau} + \left(\mathbf{v}^{\text{lab}} - \frac{\partial \mathbf{x}}{\partial \tau} \right) \cdot \text{grad}(\ ) \ . \tag{135}$$

Due to (72), (80) and (82), this is equivalent to

$$\frac{\mathcal{D}}{\mathcal{D}t} = \frac{\partial}{\partial \tau} + (u\mathbf{n} + v^j \mathbf{g}_j) \cdot \left(\frac{1}{\hat{D}} \mathbf{n} \frac{\partial}{\partial \xi} + \mathbf{g}^i \frac{\partial}{\partial \zeta^i} \right) \tag{136}$$

Since $\mathbf{n} \perp \mathbf{g}^i$ and $\mathbf{g}_j \cdot \mathbf{g}^i = \delta_j{}^i$, this is the desired result from (83).

A.2 The Divergence

For the divergence of a vector field, $\mathbf{w}$, say, we use two equivalent representations:

$$\text{div}(\mathbf{w}) = \frac{1}{J} \frac{\partial}{\partial \zeta^\nu} (J w^\nu) = \mathbf{g}^\nu \cdot \frac{\partial \mathbf{w}}{\partial \zeta^\nu} \ . \tag{137}$$

The first relation is a standard expression. To obtain the second, we replace $J w^\lambda = J \mathbf{g}^\lambda \cdot \mathbf{w}$ and use the relation

$$J \mathbf{g}^\lambda = \mathbf{g}_\mu \times \mathbf{g}_\nu \ . \tag{138}$$

Here and below, we consider $\{\lambda, \mu, \nu\}$ to be cyclic permutations of $\{0, 1, 2\}$. Thus, we get

$$\text{div}\, \mathbf{w} = \mathbf{g}^\lambda \cdot \frac{\partial \mathbf{w}}{\partial \zeta^\lambda} + \frac{1}{J} \mathbf{w} \cdot \sum_{\lambda=0}^{2} \frac{\partial}{\partial \zeta^\lambda} (\mathbf{g}_\mu \times \mathbf{g}_\nu) \ . \tag{139}$$

Carrying out the differentiation of the product in the sum of the second term and observing: (1) the definition $\mathbf{g}_\nu = \partial \mathrm{x}/\partial\zeta^\nu$ and (2) that $\{\lambda,\mu,\nu\}$ are cyclic permutations of $\{0,1,2\}$ one finds

$$\frac{\partial J\mathbf{g}^\lambda}{\partial\zeta^\lambda} = \sum_{\lambda=0}^{2} \frac{\partial}{\partial\zeta^\lambda}(\mathbf{g}_\mu \times \mathbf{g}_\nu) \equiv 0 \ , \tag{140}$$

which verifies (137)b.

To find the divergence of the velocity field in our flow problem we procede as follows: Using (74) we write $\mathrm{w} = w^0\,\hat{D}\mathrm{n} + w^i\,\mathbf{g}_i$ and then use (137)b for the normal but (137)a for the tangential component to obtain

$$\mathrm{div}(\mathrm{w}) = \frac{1}{\hat{D}}\frac{\partial}{\partial\xi}(\hat{D}w^0) + \hat{D}w^0\,\mathrm{div}(\mathrm{n}) + \frac{1}{J}\frac{\partial}{\partial\zeta^i}(Jw^i) \ . \tag{141}$$

Considering the velocity vector $\mathrm{w} = \mathrm{v}^{\mathrm{lab}}$ from (80), and noting that the sum of principal curvatures, $\kappa = \kappa_1 + \kappa_2$, of surfaces $\xi = \mathrm{const}$ obeys

$$\kappa = \mathrm{div}(\mathrm{n}) \ , \tag{142}$$

we find (85). To see (142), we observe from (137)b that $\mathrm{div}(\mathrm{n})$ is the trace of the Weingarten map $\mathbf{g}_i \rightarrow \partial\mathrm{n}/\partial\zeta^i$, whose eigenvalues are the principal curvatures, [15].

B Differential Geometric relations

B.1 The evolution equation for $\hat{\kappa}$ in 2-D

Here we work in the scaled coordinates $(\hat{\xi},\hat{\zeta})$ as introduced in (96). Recall from (142) that $\hat{\kappa} = \mathrm{div}\,\mathrm{n}$. It follows that

$$\frac{\partial\hat{\kappa}}{\partial\hat{\xi}} = \frac{\partial}{\partial\hat{\xi}}\left(\mathbf{g}^i\cdot\frac{\partial\mathrm{n}}{\partial\hat{\zeta}^i}\right) = \frac{\partial\mathbf{g}^i}{\partial\hat{\xi}}\cdot\frac{\partial\mathrm{n}}{\partial\hat{\zeta}^i} + \mathbf{g}^i\cdot\frac{\partial}{\partial\hat{\zeta}^i}\left(\frac{\partial\mathrm{n}}{\partial\hat{\xi}}\right) \ , \tag{143}$$

where the derivative $\partial/\partial\hat{\zeta}^0$ does not appear in the expression for $\mathrm{div}\,\mathrm{n}$, because $d\mathrm{n} \perp \mathbf{g}^0 = \mathrm{n}/\hat{D}$.

We use the following auxiliary relations:

$$\frac{\partial \mathbf{n}}{\partial \hat{\xi}} = -\bar{\nabla}_{\|} \hat{D} = -\mathbf{g}^i \frac{\partial \hat{D}}{\partial \hat{\zeta}^i} \tag{144}$$

and, in two dimensions,

$$\mathbf{g}^i \equiv \mathbf{g}^1 = \frac{1}{\hat{A}} \mathbf{t} \,, \tag{145}$$

$$\frac{1}{\hat{A}} \frac{\partial \hat{A}}{\partial \hat{\xi}} = \hat{\kappa} \hat{D} \,, \tag{146}$$

$$\frac{1}{\hat{A}} \frac{\partial \mathbf{n}}{\partial \hat{\zeta}^1} = \hat{\kappa} \mathbf{t} \,. \tag{147}$$

The relation (144) will be derived at the end of this appendix, while the others are equivalent to (98), (100) and (102), respectively. With these identities we transform (143) into

$$\frac{\partial \hat{\kappa}}{\partial \hat{\xi}} = \hat{A} \hat{\kappa} \mathbf{t} \cdot \frac{\partial}{\partial \hat{\xi}} \left(\frac{1}{\hat{A}} \mathbf{t} \right) - \left(\frac{1}{\hat{A}} \frac{\partial}{\partial \hat{\zeta}^1} \right)^2 \hat{D} \tag{148}$$

$$= -\left[\hat{D} \hat{\kappa}^2 + \left(\frac{1}{\hat{A}} \frac{\partial}{\partial \hat{\zeta}^1} \right)^2 \hat{D} \right] \tag{149}$$

which coincides with (106).

It remains to check (144). We decompose

$$\frac{\partial \mathbf{n}}{\partial \hat{\xi}} = \mathbf{g}^i \left(\mathbf{g}_i \cdot \frac{\partial \mathbf{n}}{\partial \hat{\xi}} \right) \tag{150}$$

and use $(\mathbf{g}_i \cdot \mathbf{n}) \equiv 0$, $(i = 1, 2)$ to obtain

$$\frac{\partial \mathbf{n}}{\partial \hat{\xi}} = -\mathbf{g}^i \left(\mathbf{n} \cdot \frac{\partial \mathbf{g}_i}{\partial \hat{\xi}} \right) \,. \tag{151}$$

Then we recall $\mathbf{g}_i = \partial \mathbf{x} / \partial \hat{\zeta}^i$ and $\partial \mathbf{x} / \partial \hat{\xi} = \hat{D} \mathbf{n}$ and conclude

$$\frac{\partial \mathbf{n}}{\partial \hat{\xi}} = -\mathbf{g}^i \left(\mathbf{n} \cdot \frac{\partial \hat{D} \mathbf{n}}{\partial \hat{\zeta}^i} \right) = -\mathbf{g}^i \frac{\partial \hat{D}}{\partial \hat{\zeta}^i} \,. \tag{152}$$

Notice that the last result is valid in two as well as in three dimensions.

Acknowledgments

R. Klein has been supported as a research visiting fellow at Princeton University by the Deutsche Forschungsgemeinschaft. D. S. Stewart has been supported through a contract with Los Alamos National Laboratory, DOE-LANL-9XG83831P1, and the National Center for Supercomputing Applications.

References

[1] Wood, W. W. and Kirkwood, J. G., *Diameter effect in condensed explosives: The relation between velocity and the radius of curvature in the detonation wave*, *J. Chem. Phys.* 22:1920-1924, (1954).

[2] Bdzil, J. B., *Steady - state two - dimensional detonation*, J. Fluid Mech., 108, 195 - 226, (1981).

[3] Stewart, D. S. and Bdzil, J. B., *The shock dynamics of stable multidimensional detonation*, Combustion and Flame, 72, 311-323, (1988).

[4] Stewart, D. S., and Bdzil, J.B., *A lecture on Detonation Shock Dynamics*, Mathematical Modelling in Combustion Science, Lecture Notes in Physics, Vol. 249, p. 17-30, Springer-Verlag Publishers, (1988).

[5] Bdzil, J. B. and Stewart, D. S., *Modeling of two-dimensional detonation with detonation shock dynamics*, Physics of Fluids, A, Vol. 1, No. 7, p. 1261, (1988).

[6] Bdzil, J. B., Fickett, W. and Stewart, D. S., *Detonation shock dynamics: A new approach to modeling multi-dimensional detonation waves*, to appear in the Proceedings of the 9th (International) Symposium on Detonation, (1990).

[7] Stewart, D. S. and Bdzil, J. B., *Examples of detonation shock dynamics for detonation wave spread applications*, to appear in the Proceedings of the 9th (International) Symposium on Detonation, (1990).

[8] Lee, H. I. and Stewart, D. S., *Calculation of linear detonation instability, one-dimensional instability of plane detonation*, Vol 216, pp 103 - 132, (1990).

[9] Witham G.B., 1959, *Linear and Nonlinear Waves*, Wiley.

[10] Fickett, W. and Davis, W. C. *Detonation*, University of California Press, (1979).

[11] Klein R., *On the dynamics of weakly curved detonations*, to appear in: Proc. of the IMA Workshop on Dynamical Issues in Combustion, Minneapolis, Minn., Eds.: A. Liñan, F.A. Williams, (1990).

[12] van Dyke, M., *Perturbation Methods in Fluid Mechanics*, Parabolic Press, Stanford, California.

[13] Bdzil J.B.,private communication.

[14] Struik J.D., 1950, *Lectures on Classical Differential Geometry*, Addison - Wesley Press, Cambridge, Mass..

[15] Millman R.S., Parker G.D., (1977), *Elements of Differential Geometry*, Prentice-Hall, Englewood Cliffs, New Jersey.

[16] Stewart D.S., Bdzil J.B., (1986), *Time-dependent twodimensional detonation: The interaction of edge rarefactions with finite length reaction zones*, J. Fluid Mech., **171**, 1–26.

[17] Bdzil J.B., (1976), *Perturbation Methods Applied to Problems in Detonation – Physics*, Proc. 6th Symp. (Intl.) on Detonation, Office of Naval Research, USGPO, Washington, ACR-221, 352-370.

[18] Buckmaster J.D., (1989) *A Theory for Triple Point Spacing in Overdriven Detonation Waves*, Comb.& Flame, 77, 219–228.

FIGURES

Figure 1.: $T(\ell)$ for plane detonation versus ℓ for $\gamma = 1.4, 1.7, 2.0$ and 2.3.

Figure 2a.: $I_1(0)$ versus θ for $\nu = 0.5$, $\gamma = 1.4, 1.7, 2.0, 2.3$.

Figure 2b.: $I_1(0)$ versus γ for $\nu = .5$, $\theta = 0, .5, 1.0$ and 2.0 and the asymptotic result evaluated with $\theta = 2.0$ shown for comparison.

Figure 2c.: $I_1(0)$ versus ν for $\gamma = 1.4$ and $\theta = 0, 1.0$ and 2.0.

Figure 3a.: The $D_n - \kappa$ relation for $\gamma = 1.4, \nu = .5$ and $\theta = 0, .5, 1.0$ and 2.0.

Figure 3b.: The $D_n - \kappa$ relation for $\gamma = 2.0, \nu = .5$ and $\theta = 0.0, 0.5, 1.0$ and 2.0.

Figure 3c.: The $D_n - \kappa$ relation for $\gamma = 1.4, \theta = 1.0$ and $\nu = 0, 0.3, 0.6, 0.9$.

Figure 3d.: The $D_n - \kappa$ relation for $\gamma = 2.0, \theta = 1.0$ and $\nu = 0, 0.3, 0.6, 0.9$.

Figure 4a.: Detonation structure for u and λ as computed from the composite expansion. $\gamma = 1.4, \nu = .5, \theta = 0.0, 0.5, 0.75$ and $\kappa = 0.02$.

Figure 4b.: Detonation structure for u and λ showing the effects of the inclusion of curvature. $\gamma = 1.4, \nu = 0.6, \theta = 1.0$ and $\kappa = 0$ and 0.01.

Figure 4c.: Detonation structure for u and λ as computed from the composite expansion. $\gamma = 1.4, \theta = 1.0, \nu = 0.0, 0.3, 0.6, 0.9$ and $\kappa = 0.01$.

Figure 4d.: Detonation structure for u and λ as computed from the composite expansion. $\gamma = 2.0, \theta = 1.0, \nu = 0, 0.3, 0.6, 0.9$ and $\kappa = 0.01$.

FIGURES

Figure 1.

$T(\ell)$ for plane detonation versus ℓ for $\gamma = 1.4, 1.7, 2.0$ and 2.3.

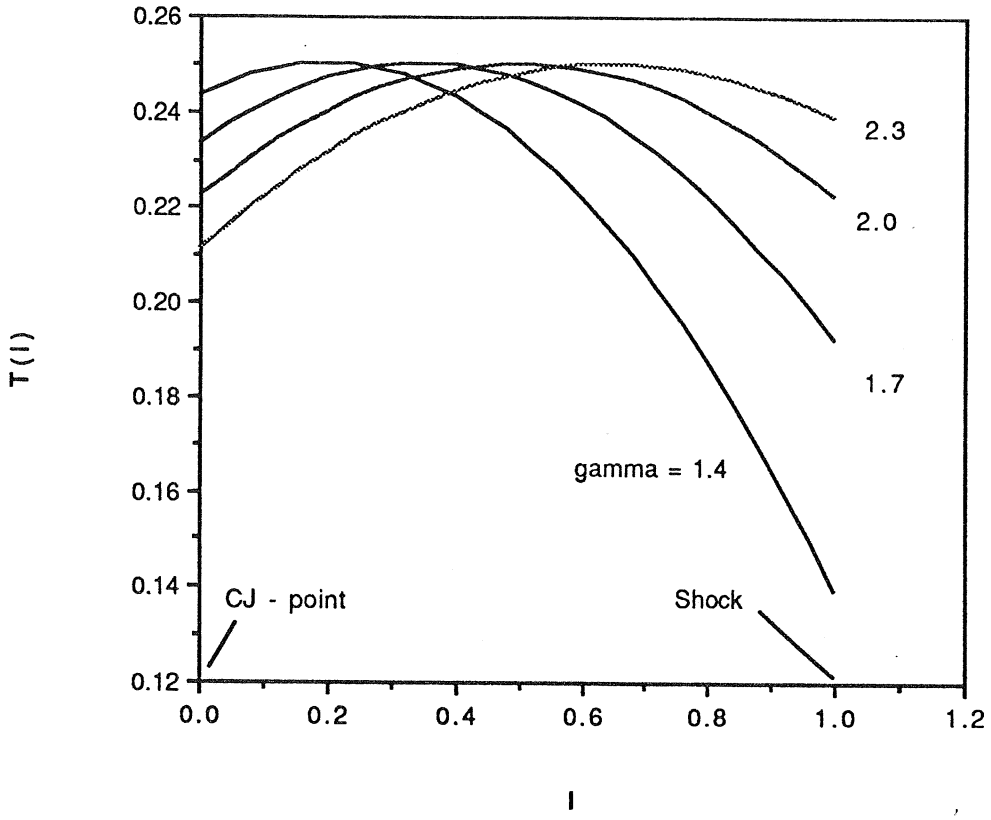

Figure 2a.

$I_1(0)$ versus θ for $\nu = 0.5$, $\gamma = 1.4, 1.7, 2.0, 2.3$.

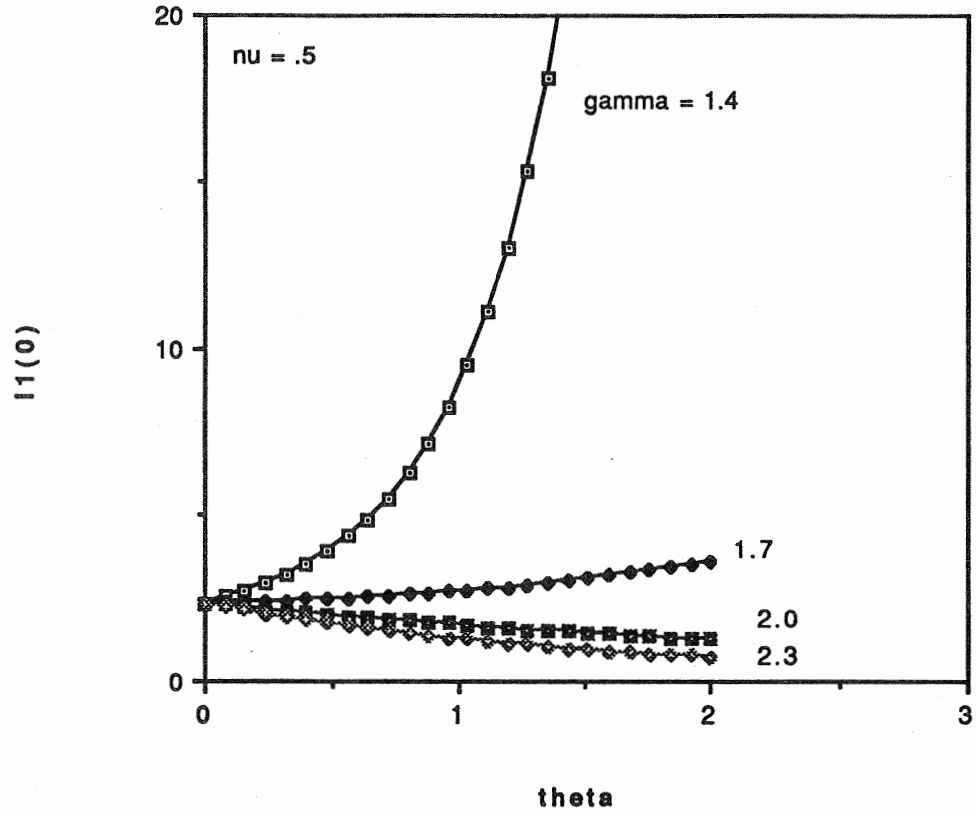

Figure 2b.

$I_1(0)$ versus γ for $\nu = .5$, $\theta = 0, .5, 1.0$ and 2.0 and the asymptotic result evaluated with $\theta = 2.0$ shown for comparison.

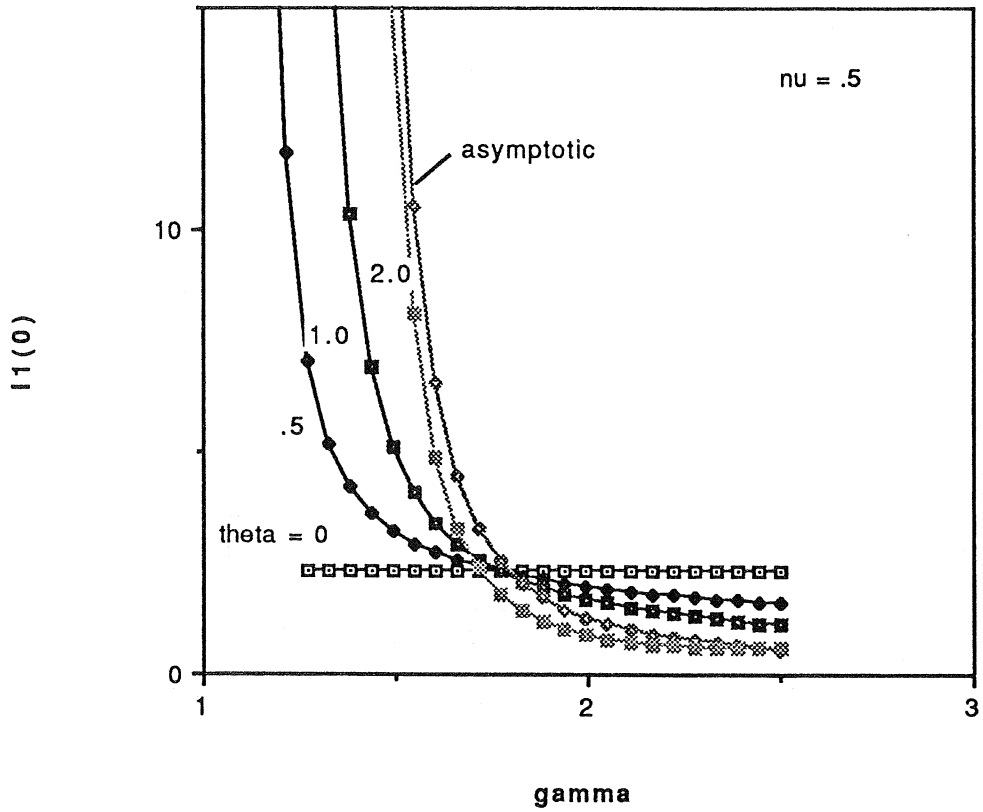

Figure 2c.

$I_1(0)$ versus ν for $\gamma = 1.4$ and $\theta = 0, 1.0$ and 2.0.

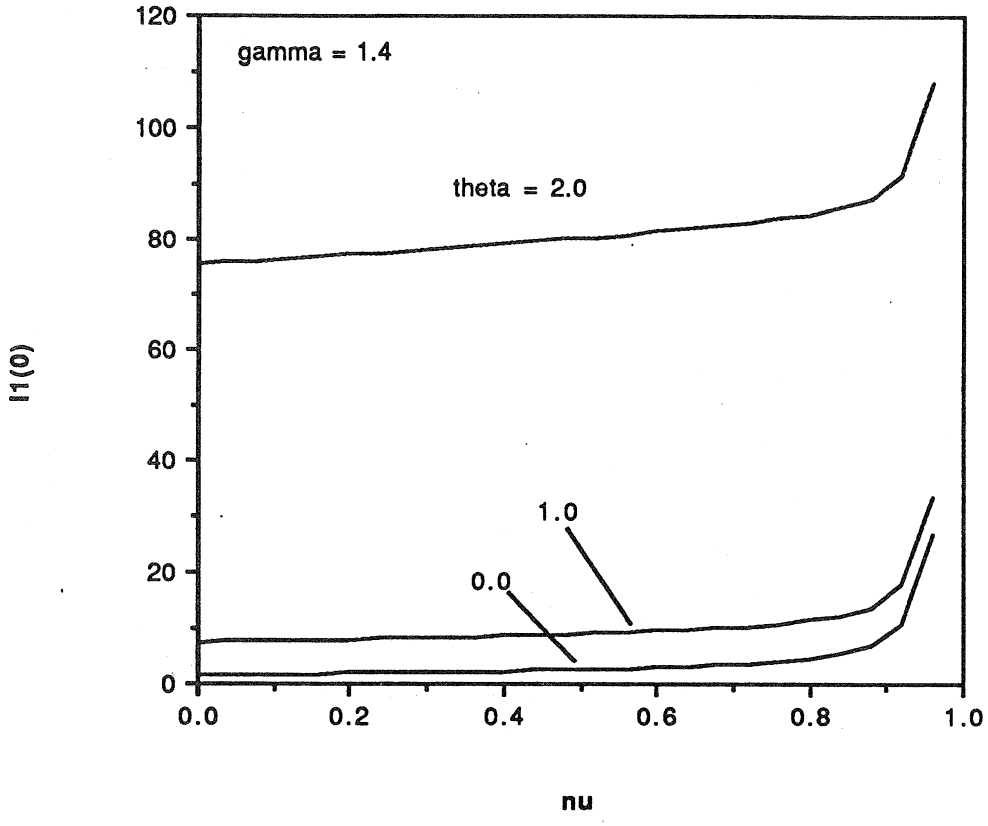

Figure 3a.

The $D_n - \kappa$ relation for $\gamma = 1.4, \nu = .5$ and $\theta = 0, .5, 1.0$ and 2.0.

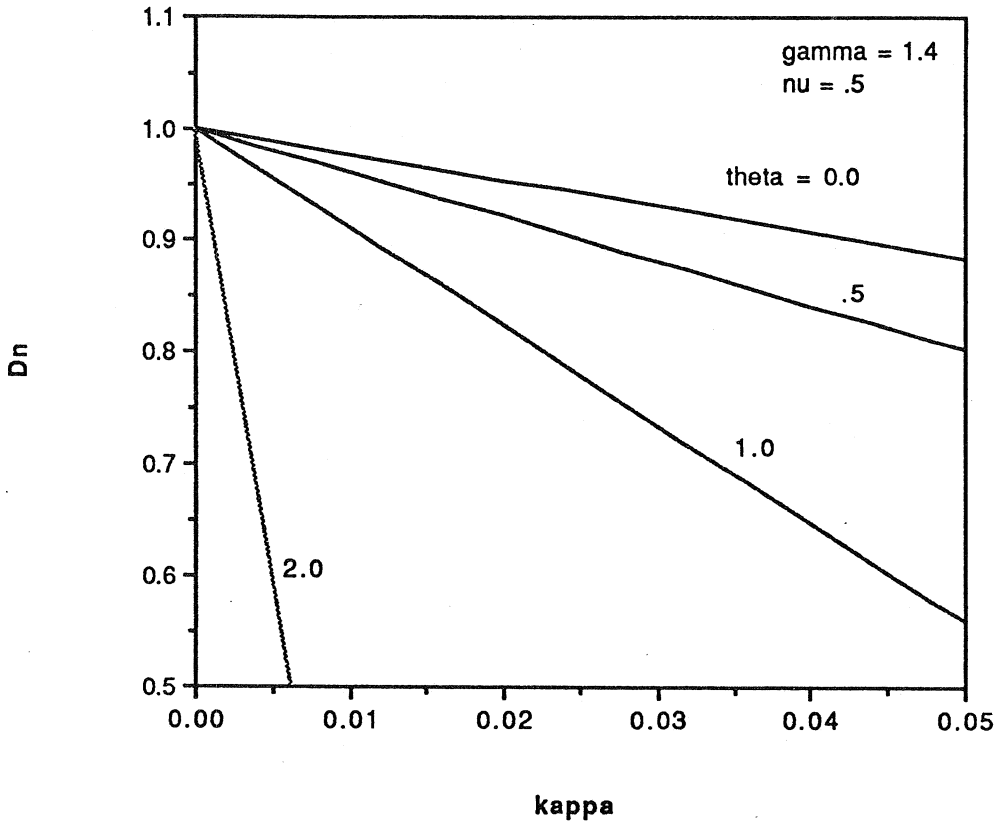

Figure 3b.

The $D_n - \kappa$ relation for $\gamma = 2.0, \nu = .5$ and $\theta = 0.0, 0.5, 1.0$ and 2.0.

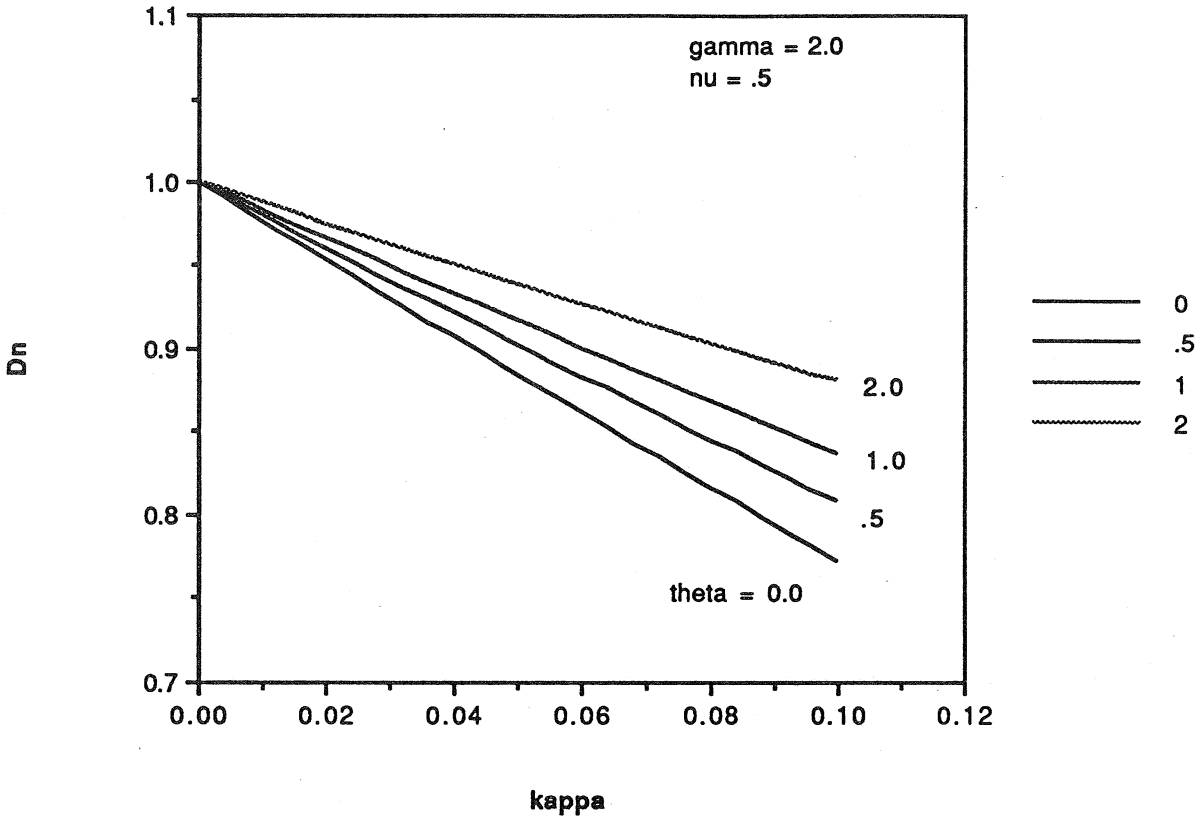

Figure 3c.

The $D_n - \kappa$ relation for $\gamma = 1.4, \theta = 1.0$ and $\nu = 0, 0.3, 0.6, 0.9$.

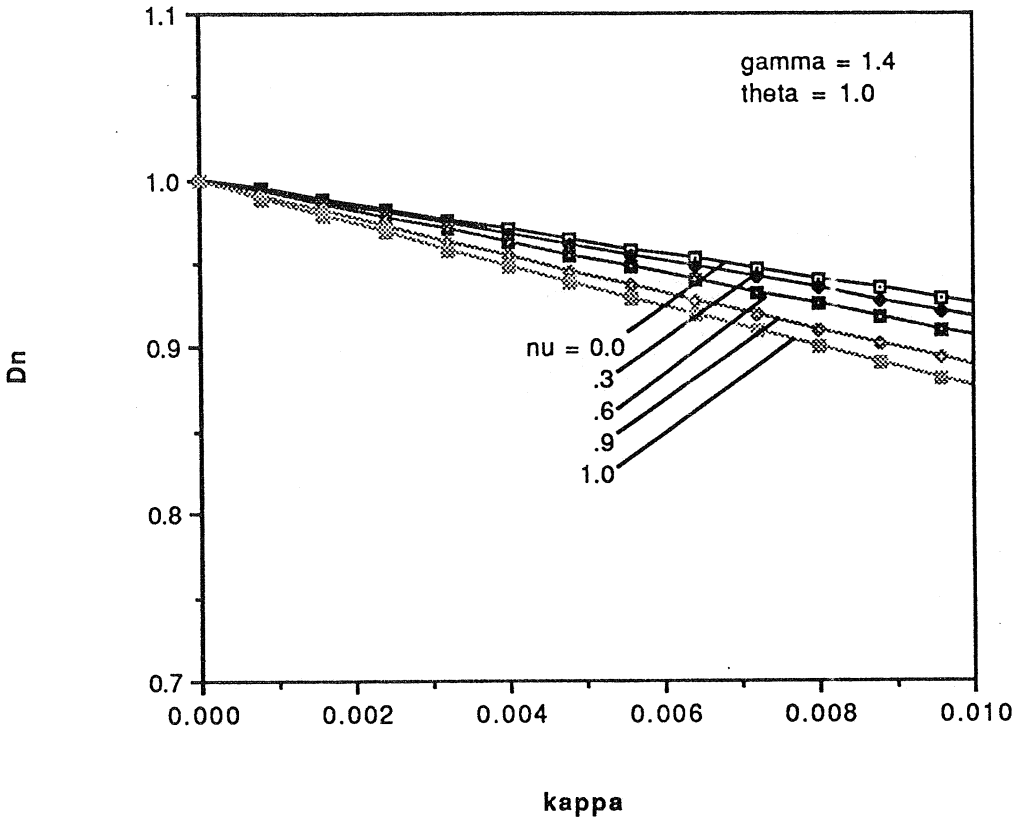

Figure 3d.

The $D_n - \kappa$ relation for $\gamma = 2.0, \theta = 1.0$ and $\nu = 0, 0.3, 0.6, 0.9$.

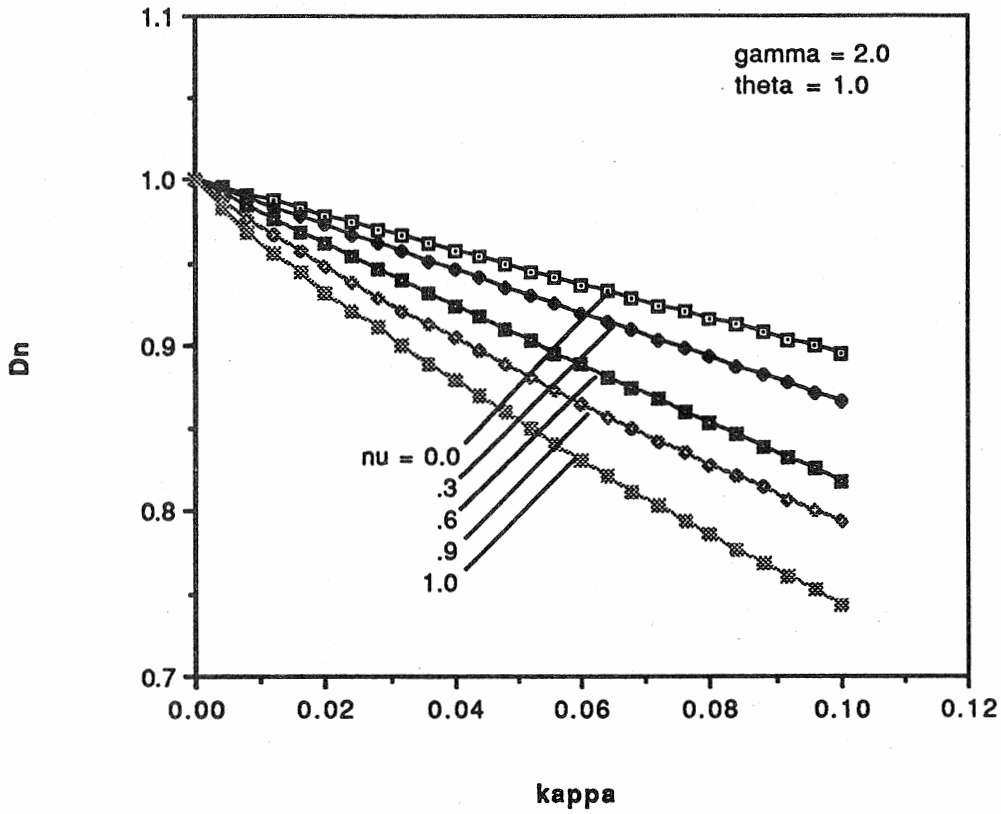

Figure 4a.

Detonation structure for u and λ as computed from the composite expansion. $\gamma = 1.4, \nu = .5, \theta = 0.0, 0.5, 0.75$ and $\kappa = 0.02$.

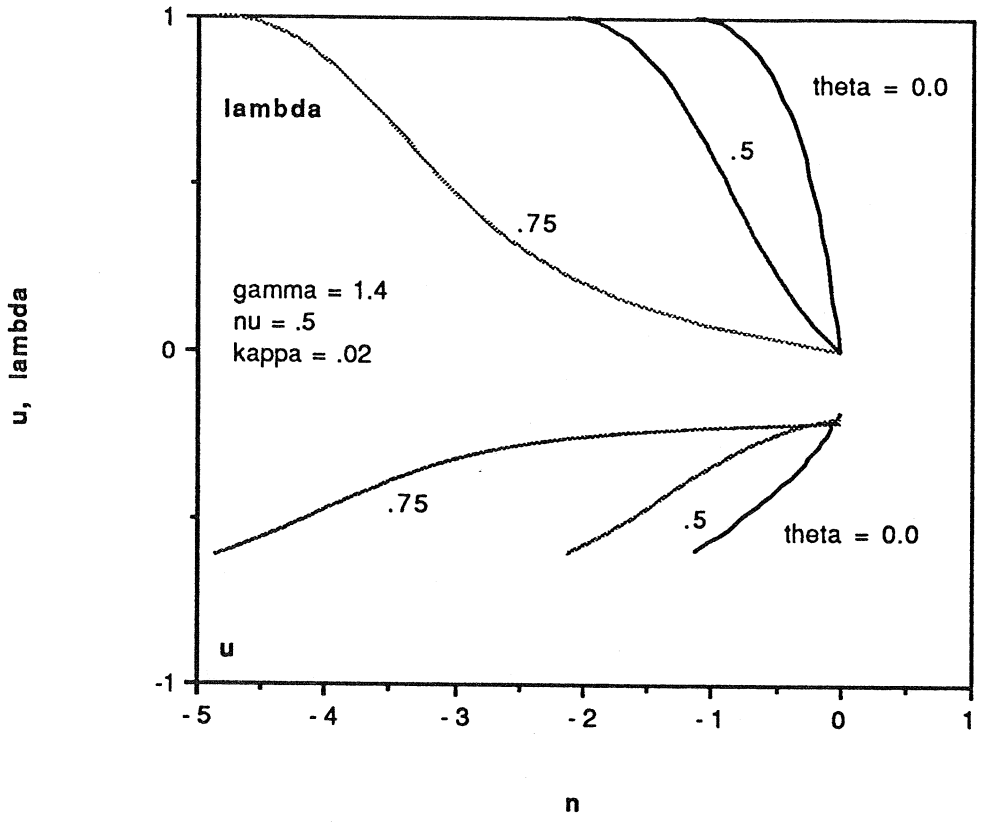

Figure 4b.

Detonation structure for u and λ showing the effects of the inclusion of curvature. $\gamma = 1.4, \nu = 0.6, \theta = 1.0$ and $\kappa = 0$ and 0.01.

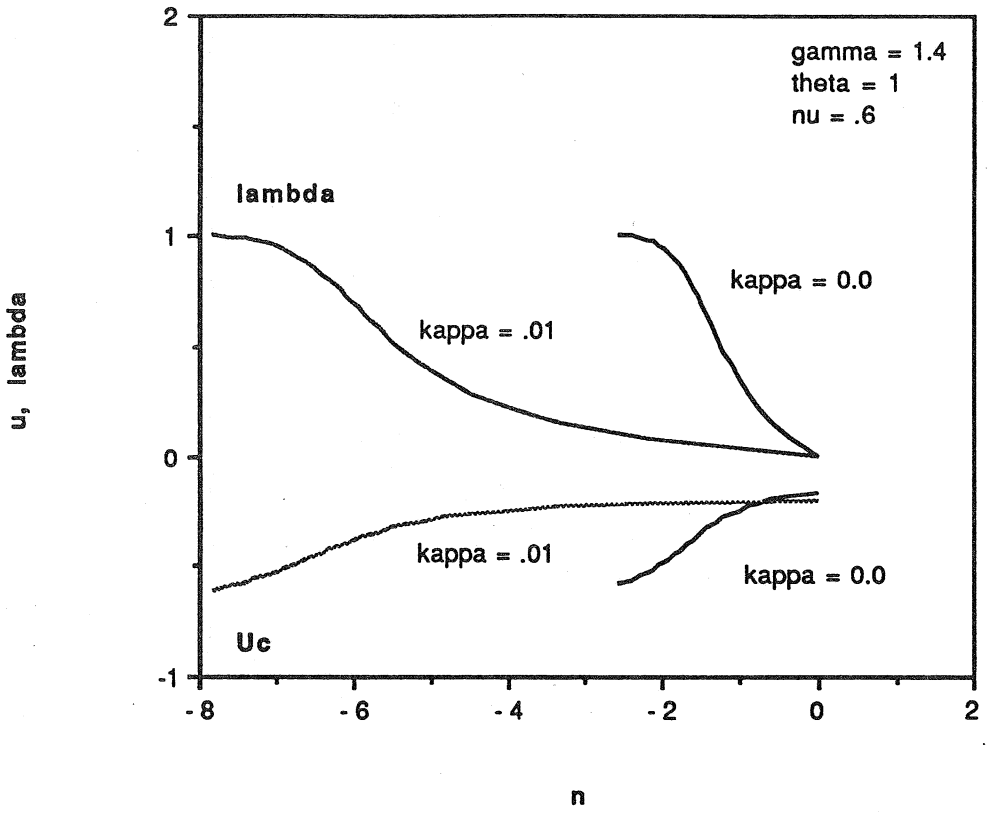

Figure 4c.

Detonation structure for u and λ as computed from the composite expansion. $\gamma = 1.4, \theta = 1.0, \nu = 0.0, 0.3, 0.6, 0.9$ and $\kappa = 0.01$.

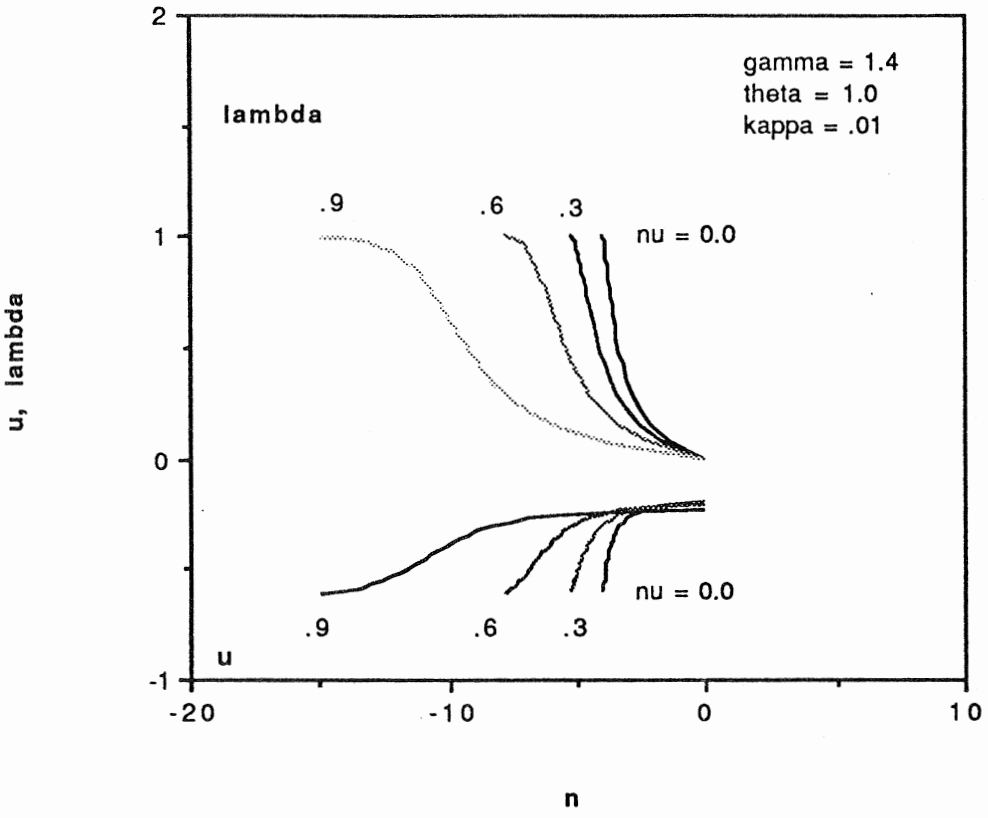

Figure 4d.
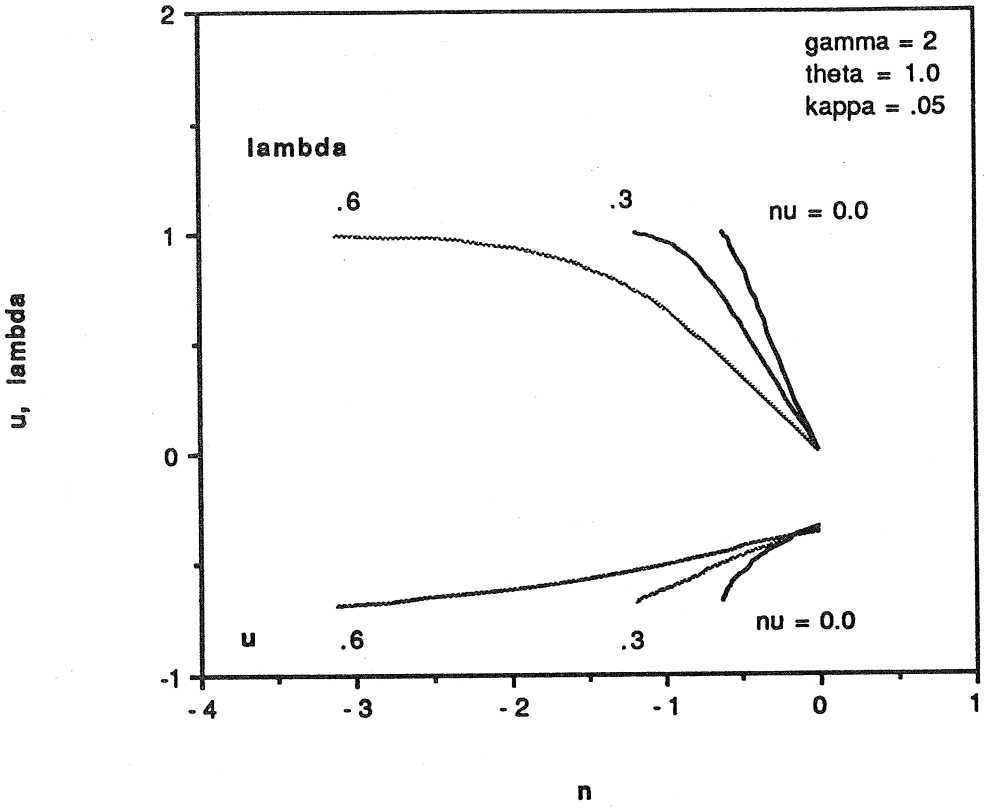
Detonation structure for u and λ as computed from the composite expansion. $\gamma = 2.0, \theta = 1.0, \nu = 0, 0.3, 0.6, 0.9$ and $\kappa = 0.01$.